มหาวิทยาลัยอุบลราชธานี

FABRICATION AND CHARACTERIZATION OF TiO_2 NANOTUBES DYE-SENSITIZED SOLAR CELLS BY ANODIZATION METHOD

SANGWORN WANTAWEE

A THESIS SUBMITTED IN PARTIAL FULFILLMENT OF THE REQUIREMENTS
FOR THE DEGREE OF DOCTOR OF PHILOSOPHY
MAJOR IN PHYSICS
FACULTY OF SCIENCE
UBON RATCHATHANI UNIVERSITY
YEAR 2013

THESIS APPROVAL

UBON RATCHATHANI UNIVERSITY

DOCTOR OF PHILOSOPHY

MAJOR IN PHYSICS FACULTY OF SCIENCE

TITLE FABRICATION AND CHARACTERIZATION OF TiO_2 NANOTUBE DYE-SENSITIZED SOLAR CELLS BY ANODIZATION METHOD

NAME MR.SANGWORN WANTAWEE

THIS THESIS HAS BEEN ACCEPTED BY

Ud. Tipparach
..... CHAIR

(ASST.PROF.DR.UDOM TIPPARACH)

Supakorn Pukird
..... COMMITTEE

(ASSOC.PROF.DR.SUPAKORN PUKIRD)

..... COMMITTEE

(DR.CHRISTIAN HERBST)

Pakut Wongwanwattana
..... COMMITTEE

(ASST.PROF.DR.PAKAWAT WONGWANWATTANA)

Jan
..... DEAN

(ASST.PROF.DR.JANPEN INTARAPRASERT)

APPROVAL BY UBON RATCHATHANI UNIVERSITY

Utith Inprasit
.....

(ASSOC.PROF.DR.UTITH INPRASIT)

VICE PRESIDENT FOR ACADEMIC AFFAIRS

FOR THE PRESIDENT OF UBON RATCHATHANI UNIVERSITY

ACADEMIC YEAR 2013

ACKNOWLEDGEMENTS

I would like to thank Mr.Wisit Withayaworakharn who is the director of Rajapachanukou 29 Sisaket province for supporting my Ph.D.program at department of Physics, Faculty of Sciences, Ubon Ratchathani University. In addition, I appreciate my advisor, Asst.Prof.Dr.Udom Tipparach, for coaching, teaching, helping and valuable guidance through three and half years with thesis work. I would like to thank the thesis committee, Assoc.Prof.Dr.Supakorn Pukird, Dr.Christian Herbst, for our suggestions and kindness. Especially, I would like to thank the external committee member, Asst.Prof.Dr.Pakawat Wongwanwattana from Department of Physics, Faculty of Science, Ubon Ratchathani Rajabhat University for his comments and suggestions.

In addition, I would like to thank all faculty members in Department of Physics, Department of Chemistry, Faculty of Science, Ubon Ratchathani University for their teaching and technical supports for this work.

Finally, I thank my parents and my wife for encouragement supports. I would not be here today without them.

Sangworn Wantawee

(Mr.Sangworn Wantawee)

Researcher

บทคัดย่อ

ชื่อเรื่อง : การผลิตและการศึกษาลักษณะบ่งชี้ของเซลล์แสงอาทิตย์สีย้อมไวแสงท่อนาโนไททาเนียมไดออกไซด์โดยวิธีการแอโนไดเซชัน

โดย : สังวร วรรณทวี

ชื่อปริญญา : ปรัชญาดุษฎีบัณฑิต

สาขาวิชา : ฟิสิกส์

ประธานกรรมการที่ปรึกษา : ผู้ช่วยศาสตราจารย์ ดร.อุดม ทิพราช

ศัพท์สำคัญ : ท่อนาโนไททาเนียมไดออกไซด์ เซลล์แสงอาทิตย์สีย้อมไวแสง แอโนไดเซชัน

ท่อนาโนไททาเนียมไดออกไซด์ถูกสังเคราะห์และถูกใช้เพื่อผลิตเซลล์แสงอาทิตย์สีย้อมไวแสง วิธีการแอโนไดเซชันถูกใช้เพื่อเตรียมท่อนาโนไททาเนียมไดออกไซด์ เงื่อนไขสำหรับการแอโนไดเซชันประกอบด้วยการศึกษาผลของค่า pH และผลของค่าความต่างศักย์ ลักษณะบ่งชี้ของท่อนาโนไททาเนียมไดออกไซด์ถูกศึกษาด้วยกล้องจุลทรรศน์อิเล็กตรอนแบบส่องกราด (SEM) เทคนิคการเลี้ยวเบนรังสีเอ็กซ์ (XRD) และเครื่อง UV-vis spectrometer เฟสของท่อนาโนไททาเนียมไดออกไซด์เป็นอนาเทสและมีเส้นผ่านศูนย์กลางระหว่าง 90 nm - 200 nm สัมพันธ์กับความต่างศักย์ 40, 50, 60 และ 70 V ตามลำดับ ท่อนาโนไททาเนียมไดออกไซด์ถูกใช้เป็นเวิคคิ้งอิเล็กโทรดสำหรับการทำเซลล์แสงอาทิตย์สีย้อมไวแสง การวัด I-V cuves ของเซลล์ถูกทดสอบโดย eDAQ potentiostat เซลล์แสงอาทิตย์สีย้อมไวแสงที่เงื่อนไขความต่างศักย์มีประสิทธิภาพร้อยละ 4.21, 4.77, 6.10 และ 6.89 ตามลำดับ ภายใต้ความเข้มแสง 60 mW/cm^2

ABSTRACT

TITLE : FABRICATION AND CHARACTERIZATION OF TiO_2 NANOTUBE DYE-SENTIZED SOLAR CELLS BY ANODIZATION METHOD

BY : SANGWORN WANTAWEE

DEGREE : DOCTOR OF PHILOSOPHY

MAJOR : PHYSICS

CHAIR : ASST.PROF.UDOM TIPPARACH, Ph.D.

KEYWORDS : TiO_2 NANOTUBES / DYE-SENSITIZED SOLAR CELLS / ANODIZATION

Titanium dioxide nanotubes were synthesized and used to fabricate dye-sensitized solar cells. Anodization method was used to prepare TiO_2 nanotubes. The anodization conditions include the effect of pH values and anodization voltages. Scanning electron microscopy (SEM), X-ray diffraction (XRD) and UV-visible Spectrometer were used to characterize of the prepared samples. The phase of TiO_2 nanotubes is anatase and the diameters of the tubes are in the range of 90 nm - 200 nm corresponding with 40, 50, 60 and 70 V, respectively. The specimens were used as working electrodes for making dye-sensitized solar cells. The measurements of the I-V characteristic cuves were carried out by using eDAQ potentiostat. The photoconversion efficiencies of dye-sensitized solar cells made of the working electrodes obtained from of 40, 50, 60 and 70 V were 4.21%, 4.77%, 6.10% and 6.89%, respectively, under irradiation of 60 mW/cm^2.

CONTENTS

CONTENTS (CONTINUED)

LIST OF TABLE

LIST OF FIGURES

LIST OF FIGURES (CONTINUED)

LIST OF FIGURES (CONTINUED)

FIGURES **PAGE**

CHAPTER 1

INTRODUCTION

Since the industrial revolution began in the 18th century, fossil fuels in the form of coal, oil, and natural gas have powered the technology and transportation networks that drive society. However, continuing to power the world from fossil fuels threatens our energy supply and put enormous strains on the environment. The world's demand for energy is projected to double by 2050 in response to population growth and industrialization of developing countries [1]. The vast uses of fossil fuel, causing environmental pollution and global warming, have led us to focus on the renewable energy sources for the future [2]. One of the biggest challenges ahead of human kind is to replace the fossil fuel with renewable energy sources while keeping pace with the worldwide increasing thirst for energy because of increasing population and rising demand from developing countries. This challenge has to be answered with a low-cost solution using abundantly available raw materials. The sun is an obvious source of clean and cheap energy, already used by nature to sustain almost all life on Earth. Therefore harnessing the power of the Sun with photovoltaic technologies appears to be the only reasonable large scale answer to the energy challenge. Up to now, commercially available photovoltaic technologies are based on inorganic materials such as Si and GaAs, which require high costs and highly energy consuming preparation methods. In addition, several of those materials, like CdTe, are toxic and have low natural abundance. Organic photovoltaic can avoid those problems. The efficiencies of organic-based photovoltaic cells are still at the moment a long way behind those obtained with purely inorganic based photovoltaic technologies [3].

Titanium dioxide is an attractive semiconductor material because of its photocatalytic activity and its application in the areas of electronics, gas sensors, dye sensitized solar cells (DSSCs), hydrogen generation, photovoltaics, fuel cells, photochemistry, photoelectrolysis, biology, environmental purification and self-cleaning materials. The photocatalytic activity of a photocatalyst is due to the production of excited electrons in the conduction band of the semiconductors (SCs)

along with corresponding positive holes in the valence band by the absorption of UV and/or visible photons. The photocatalytic efficiency of the anatase TiO_2 is known to be more effective than that of other polymorphs of titania. Some nanostructures like nano powders and nanotubes increase the efficiency of these applications of TiO_2 because of their high surface-to-volume ratios. Compared with nanoparticles, nanotubes can provide higher aspect ratio due to their central hollow structures [4].

The properties of TiO_2 materials are strongly related to the control of desired morphology, specific surface area, composition, size, crystallinity and porosity for various applications mentioned above. TiO_2 materials with diverse morphologies, such as mesoporous films, spheres, beads, wires, rods, submicro-rings, as well as tubular structures, have been reported in recent years. Of particular interest is tubular structures which may contribute simultaneously to the extension of porosity, specific surface area, electrical transport and light absorption [5]. Highly ordered TiO_2 nanotube arrays have attracted extensive attention due to their large surface area, low electron recombination and charge-transport properties. Compared with nanoparticles, TiO_2 nanotube arrays are considered to be superior chemical materials because they form one-dimensional channels for carrier transport. They are of considerable interest for applications in water photolysis, gas sensors, solar energy cells, biomedical catalysts, and so on. The physical and chemical properties of their structures depend on geometric features such as tube length, pore diameter and wall thickness, which also have important effects on device efficiency. Therefore, a variety of preparation routes have been used to fabricate TiO_2 nanotubes: hydrothermal synthesis, template synthesis, sol–gel methods and anodic oxidation. However, anodic oxidation can produce vertically ordered TiO_2 nanotubes in which the amount of e−/h+ recombination is reduced. There are three kinds of crystal phases found in titania: anatase, rutile and brookite. The properties of titania depend on its crystallinity and phase type. Anatase is preferable to rutile for dye-sensitized solar cells (DSSCs), whereas rutile is suitable for gas sensors and water photolysis. The annealing conditions for TiO_2 nanotube arrays have also been investigated by a number of researchers [6].

In the future, any further increase in existing DSSC efficiency largely relies on new dyes that could absorb both high- and low-energy photons. A few articles have

also reported that the nanoarchitecture comprising an array of highly ordered, vertically aligned titania nanotubes grown by anodic oxidation of titanium offers longer electron diffusion lengths and shorter electron transport time constants superior to randomly oriented titania nanoparticle films [7].

However, to the best of our knowledge, very few studies on electrochemical etching of titanium to prepare highly ordered TiO_2 nanotube arrays in organic solvents has been reported. In the present study, there are four different fluorides based electrolyte solutions and studied their effect on the TiO_2 nanotube length as a function of varying anodizing conditions like reaction time, and annealing before/after anodization [6-7]. A dye-sensitized solar cell is a class of photoelectrochemical cells, which converts sunlight to electric energy directly. DSSCs offer moderate conversion efficiency with other advantages, such as low production cost, easy scale-up, good performance under weak/diffuse light, and compatibility with building window glass and flexible substrates [8]. A variety of methods have been developed to synthesize TiO_2 nanotubes including electrochemical anodization [9], sol–gel method [10], and hydrothermal process [11]. Among the fabrication approaches, the electrochemical anodization is a very promising one, which was successfully applied in the preparation of tailored porous structures of Al_2O_3 and Si, and more recently of self-organized, vertically aligned TiO_2 nanotube arrays. Formation of self-organized TiO_2 nanotubes is the result of a fine balance between the electrochemical processes (field assisted oxidation of Ti metal to form titanium dioxide and dissolution of Ti metal) and chemical dissolution of Ti and TiO_2 [12].

Electrochemical anodization is low cost and convenient method for modification of surface structure of different metal oxides. At first, electrochemical anodization was applied for obtaining porous alumina. Then the anodization method was adopted to obtain porous structures of TiO_2. Titania nanotubes were sensitive mainly towards hydrogen. The enhancement of characteristics of metal oxide gas sensors is possible by addition of other metals as dopants or mixtures. One further application of TiO_2 nanotubes is in photoanodes for dye-sensitized solar cells, where the straight tubular structure acts as transparent electron conductor and, at the same time, hosts dye molecules responsible for light absorption. In this context, titania nanotubes are required to posses high specific surface to obtain high dye uptake and,

as a consequence, high optical density of the photoanode in the range of light absorption of the dye [13]. Since the fabrication by Ti anodization was realized, the TiO_2 nanotube arrays have demonstrated perspective applications in a variety of fields. When used in the DSSCs, the TiO_2 nanotubes are expected to have advantages over TiO_2 particles. First, their one-dimensional structure can reduce the transport dimensionality and recombination of the photoinjected electrons. Second, their tubular structure provides large area for hosting dye molecules and receiving illumination [14].

In this work, we intended to synthesize Titanium Dioxide (TiO_2) nanotubes by anodization method. For making dye-sensitized solar cells, we also investigated the anodization condition such as pH values and anodization voltages. The nanotubular layer was obtained by Ti metal anodization in an electrolyte consisting of a mixture of oxalic acid ($H_2C_2O_4$), ammonium fluoride (NH_4F), and sodium sulphate (Na_2SO_4) with different pHs and an electrolyte consisting of a mixture of $C_2H_6O_2$, NH_4F, and DI water under the applied voltages of 40 and 70 V. The characterization of TiO_2 nanotubes films is used by X-ray diffraction (XRD), scanning electron microscopy (SEM) and UV-vis spectrometer. Finally, we tested dye-sensitized solar cell by using TiO_2 nanotubes as a working electrode.

The objectives of this work are to synthesize TiO_2 nanotubes by anodization method and to test the efficiency of dye-sensitized solar cell by using TiO_2 nanotubes as a working electrode.

CHAPTER 2

THEORETICAL BACKGROUND AND LITERATURE REVIEW

2.1 Semiconductivity

Materials are divided into three groups depending on their electrical conductivity. The best conducting materials are conductors, materials with very low electrical conductivity are insulators, and materials having electrical conductivity between conductors and insulators are semiconductors. Furthermore, the property of materials can be depicted in terms of the energy bands as shown in Figure 2.1 The electronic structure of a semiconductor plays a key role in semiconductor photocatalysis. Unlike conductors, semiconductors have valence band (VB) and conduction band (CB) overlap. When semiconductors are excited by photons with energy equal to or higher than their band gap energy, electrons are promoted from VB to CB [15].

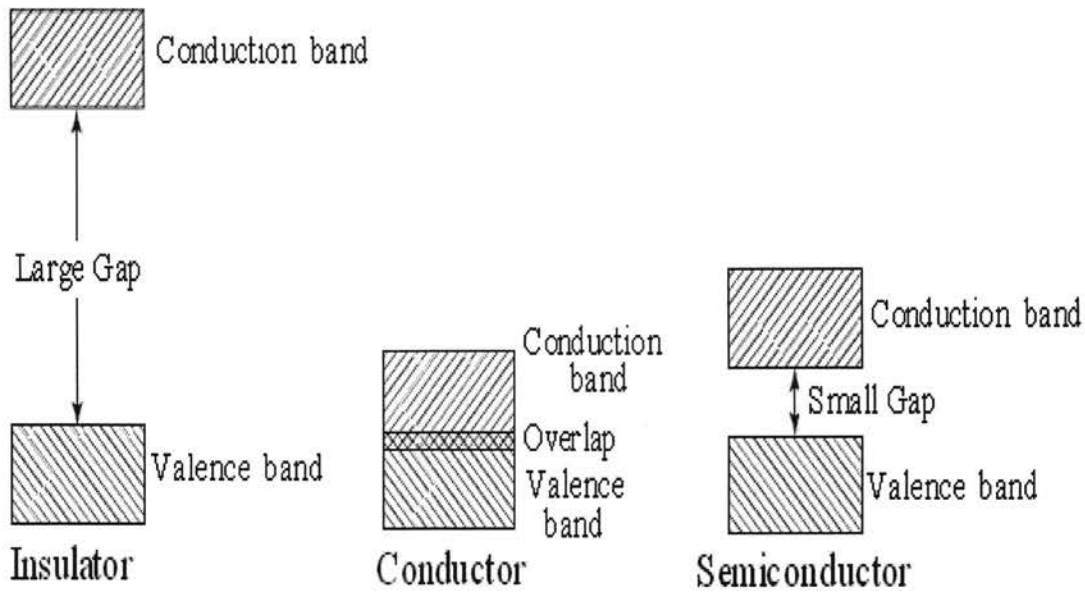

Figure 2.1 the comparison of the band structure of insulator, conductor and semiconductor.

Charge carriers in a semiconductor can be negative or positive, or both when an electron moves from the valence band into the conduction band, it leaves behind a vacant site, called a hole, in the otherwise filled valence band. This hole (electron-deficient site) appears as a positive charge and acts as a charge carrier in the sense that a free electron from a nearby site can transfer into the hole. Whenever an electron does so, it creates a new hole at the site it abandoned. Thus, the net effect can be viewed as the hole migrating through the material in the direction opposite the direction of electron movement [16]. In a pure crystal containing only one element or one compound, these are equal numbers of conduction electron and hole pair, in an external electric field, the holes move in the direction of the field, and the conduction electrons move in the direction opposite the field as shown in Figure 2.2.

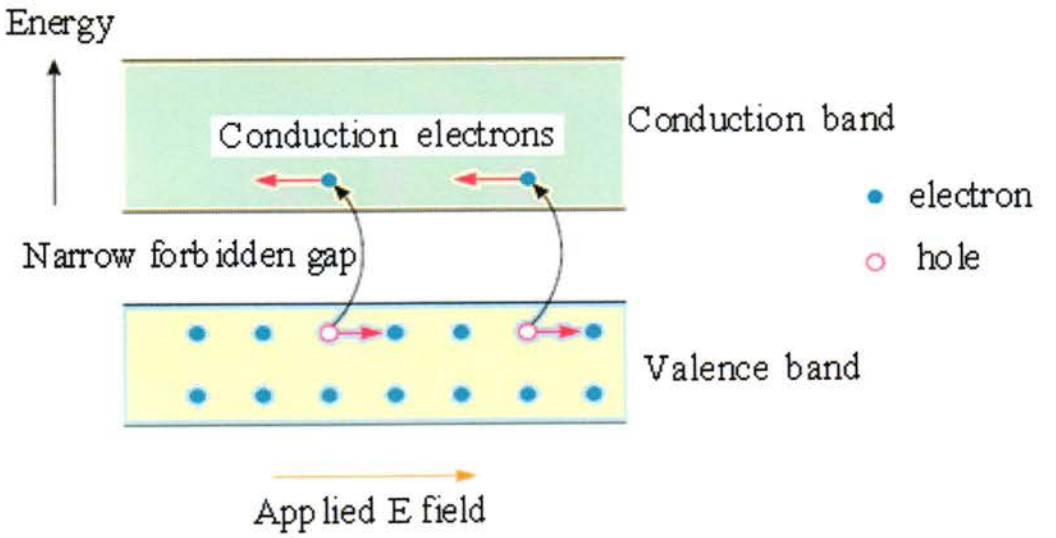

Figure 2.2 Movement of charges in an intrinsic semiconductor.

2.2 Titanium dioxide

2.2.1 TiO_2 structures and properties

Titanium dioxide (TiO_2) exists as three different polymorphs; anatase, rutile and brookite. The primary source and the most stable form of TiO_2 is rutile. All three polymorphs can be readily synthesised in the laboratory and typically the metastable anatase and brookite will transform to the thermodynamically stable rutile

upon calcination at temperatures exceeding ~600 °C. In all three forms, titanium (Ti^{4+}) atoms are co-ordinated to six oxygen (O^{2-}) atoms, forming TiO_6 octahedra. Anatase is made up of corner (vertice) sharing octahedra which form (001) planes (Figure 2.3a) resulting in a tetragonal structure. In rutile the octahedra share edges at (001) planes to give a tetragonal structure (Figure 2.3b), and in brookite both edges and corners are shared to give an orthorhombic structure (Fig.2.3c). Titanium dioxide is typically an n-type semiconductor due to oxygen deficiency. The band gap is 3.2 eV for anatase phase, 3.0 eV for rutile phase, and ~3.2 eV for brookite phase. Anatase and rutile are the main polymorphs and their key properties are summarized in Table 2.1. TiO_2 is the most widely investigated photocatalyst due to high photo-activity, low cost, low toxicity and good chemical and thermal stability. In the past few decades there have been several exciting breakthroughs with respect to titanium dioxide [17].

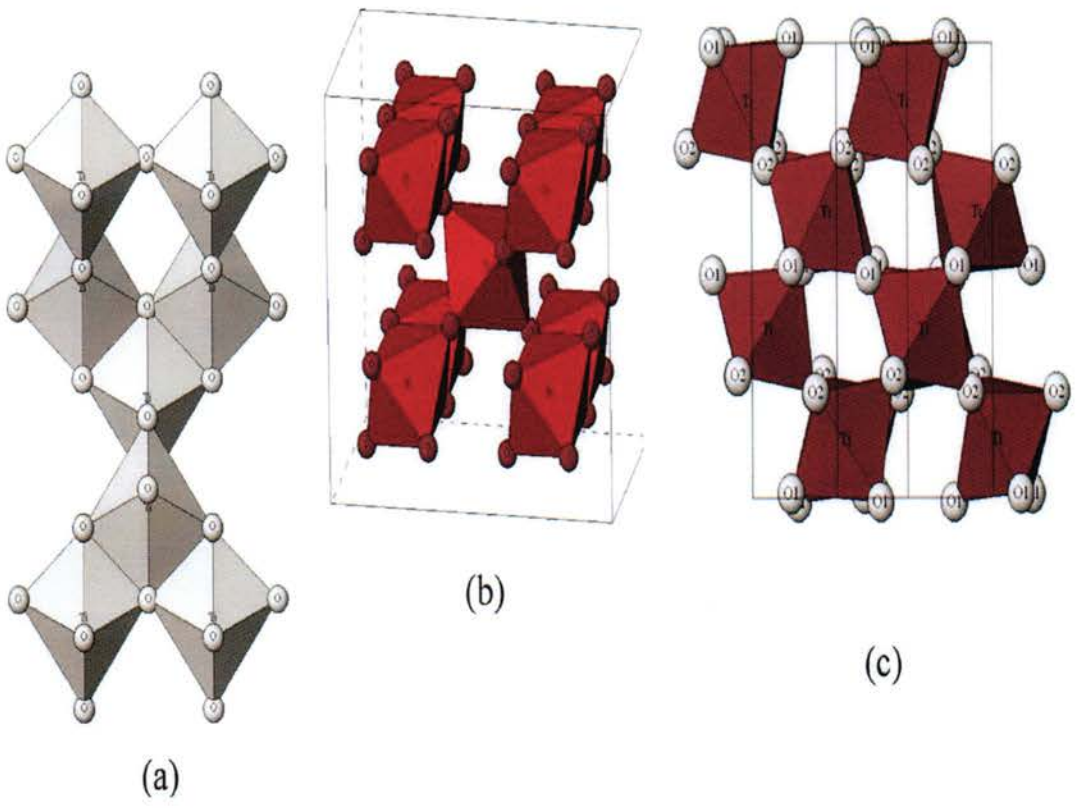

Figure 2.3 Crystalline structures of titanium dioxide (a) anatase, (b) rutile, (c) brookite [17].

Table 2.1 Physical and structural properties of anatase and rutile TiO_2 [17-18].

Property	Anatase	Rutile
Molecular weight (g/mol)	79.88	79.88
Melting point (°C)	1825	1825
Boiling point (°C)	2500-3000	2500-3000
Light absorption (nm)	< 390	< 415
Mohr's Hardness	5.5	6.5 - 7.0
Refractive index	2.55	2.75
Dielectric constant	31	114
Crystal structure	Tetragonal	Tetragonal
Lattice constant (Å)	a = 3.78	a = 4.59
	c = 9.52	c = 2.96
Density (g/cm^3)	3.79	4.13
Ti - O bond length (Å)	1.94 (4)	1.95 (4)
	1.97 (2)	1.98 (2)

The crystal structure of anatase and rutile is tetragonal; while the brookite has an orthorhombic structure as shown in figure 2.4. Since brookite is less studied and does not play a considerable role in many of the titanium dioxide applications, we will focus only on the anatase and rutile phases.

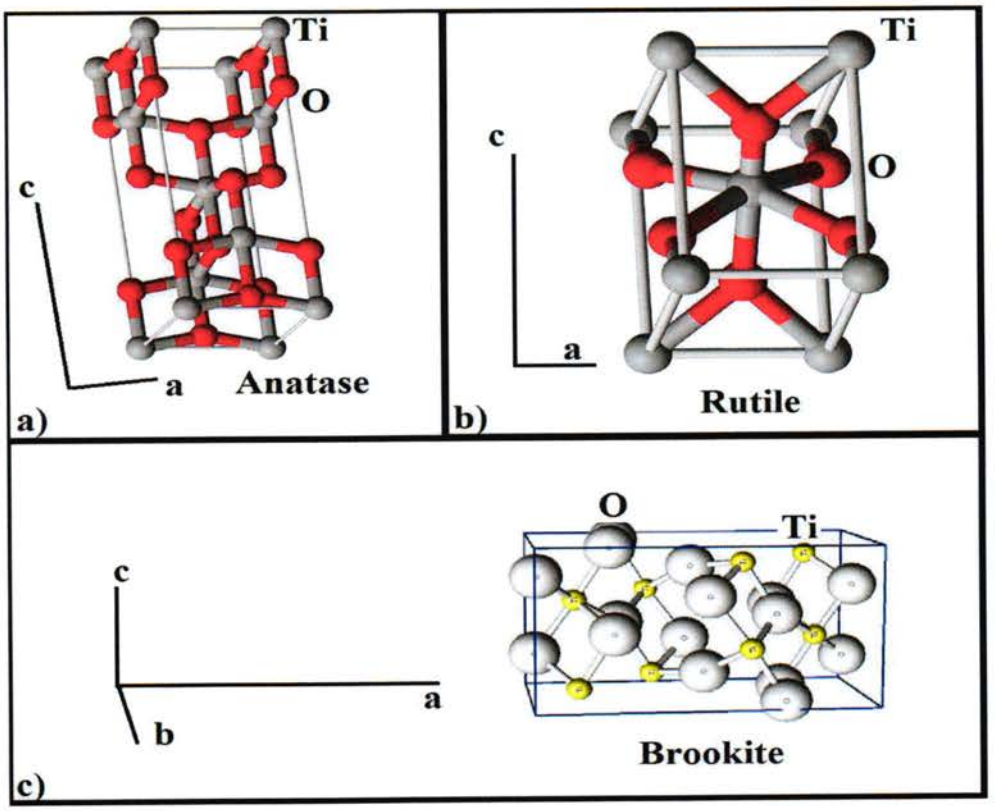

Figure 2.4 Geometrical illustration of the crystal structure of anatase, rutile and brookite [18].

2.2.2 The photocatalytic of Titanium dioxide

Titanium dioxide (TiO_2) also known as titania, is an important commercial product that has been used in many commercial applications that range from industrial (paint and pigment) to cosmetic (skin-care product). On a research level, it is interested for water splitting, solar photovoltaic cells and water or air remediation. Many studies used TiO_2 as photocatalysts for water splitting to produce hydrogen. TiO_2 have three crystalline forms such as rutile, anatase and brookite. However, all of these anatases show a higher photocatalytic activity. Even through the crystal lattices of rutile and anatase are similar, but there are a few significant differences. Band gaps of Rutile and anatase are 3.02 eV and 3.2 eV, respectively. Rutile and anatase also have different numbers of active site. A common observation is that for anatase good photocatalytic activity is observed, while rutile shows good photocatalytic activity in some and almost zero activity in other studies. The small

difference of band gap between rutile and anatase cannot explain their different activity. A main difference is their recombination rate of photoinduced electrons and holes that anatase is higher than rutile. Often heat treatment at high temperatures is used to obtain the rutile phase, resulting in the irreversible loss of surface hydroxylation and increased crystal growth, both of which decrease the photcatalytic activity of TiO_2. On the other hand a combination of the two crystal phases can lead to an enhancement of the photocatalytic activity. The recombination of anatase and rutile is the P25 powder from Degussa which has become a reference powder photocatalyst. Photoinduced processes on TiO_2 are characterized by the presence of photoinduced phenomena. All these photoinduced processes originate from the semiconductor band gap as shown in Figure 2.5.

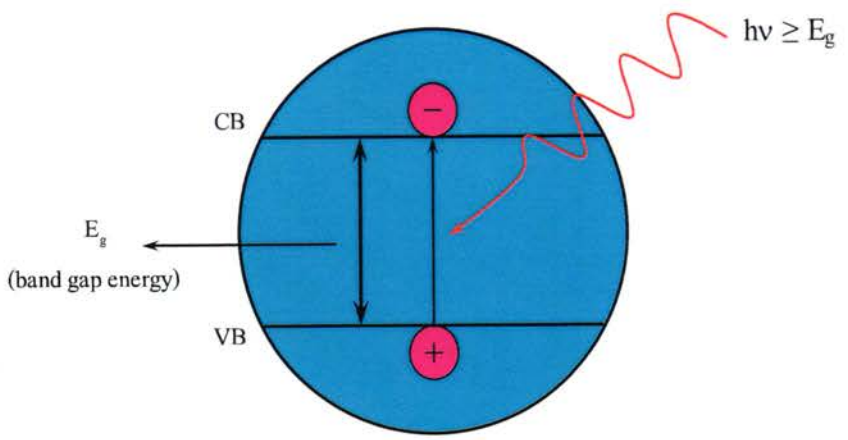

Figure 2.5 Photoinduced processes on TiO_2 [15].

When photons have a higher energy than this band gap, they can be absorbed and an electron is promoted to the conduction band, leaving a hole in the valence band. This excited electron can either be used directly to create electricity in photovoltaic solar cells or drive a chemical reaction, which is called photocatalysis. A special phenomenon was recently discovered: trapping of holes at the TiO_2 surface causes a high wettability and is termed 'photoinduced superhydrophilicity' (PSH). All photoinduced phenomena involve surface bound redox reactions. TiO_2 mediated photocatalytic reactions are gaining nowadays more and more importance and this is reflected in the increasing number of publications that deal with theoretical aspects

and practical applications of these reactions as illustrated in Figure 2.5. By far, the most active field of TiO_2 photocatalysis is the photodegeneration of organic compounds.

2.3 Formation of TiO_2 nanotube arrays

2.3.1 Electrochemical Anodization method

Electrochemical anodization is a process of oxidizing a bare metallic surface. This oxidization process is done by the effect of applied electric field between this metallic surface and another chemically inert metal when both are immersed in a given electrolyte. The anodization process acts to uniformly oxidize the surface of the required metal. The oxide layer is controlled by many factors; in most cases, the main factors that control the oxide layer properties are the applied voltage, the electrolyte, and the duration of the anodization process. The anodization can be done through two different setups, two-electrode anodization cell or three-electrode anodization cell as shown in Figure 2.6.

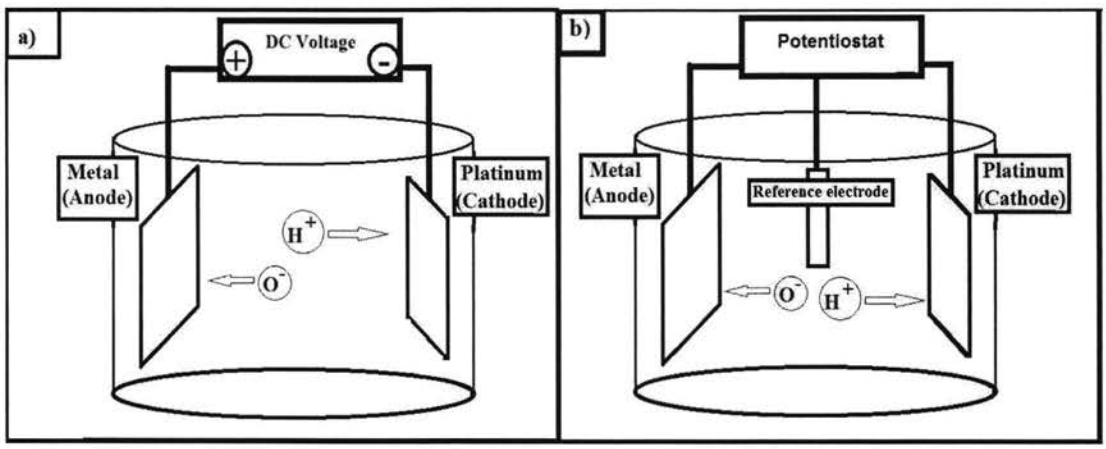

Figure 2.6 Schematic diagrams for a) two electrodes and b) three electrodes anodization cell [18].

In the two-electrode cell, the positive terminal of a DC power supply is connected to the given metal which acts as the anode, and the negative terminal is connected to platinum mesh which acts as the cathode. Both anode and cathode are immersed in a specific electrolyte. Under appropriate voltage, when the DC power

supply is switched on, an electric field is generated in the electrolyte which pulls the positive ions (hydrogen ions) towards the cathode and the negative ions (oxygen ions) towards the anode. At the metal surface, the oxygen ion loses its electrons to the metal atoms and bond with these atoms to form a metal oxide. After the first wave of oxygen ions reach the metallic surface, a metal oxide layer forms and covers the metallic surface. The successive waves of oxygen ions have to diffuse through the recently formed oxide layer to reach the metallic surface underneath and react with those atoms to form another oxide layer under the older one. In time, the oxide layer grows and becomes thick, so the diffusion rate is slower and weaker. If this process continues, only the oxide layer will reach a critical thickness where it is impossible for oxygen ions to diffuse to reach the metallic surface. Another process which keeps the anodization reaction going is the dissolution of the oxide layer in the electrolyte. Most electrolytes dissolve metal oxide; in this case, the first layer of the oxide to dissolve is the oldest layer or the first layer formed.

As a result of these two combating reactions, oxidation at the metallic surface and dissolutions at the oxide surface, the thickness of the oxide layer is controlled. On the other hand the positive hydrogen ions are pulled toward the cathode where it receives electrons and hydrogen gas is formed in the form of bubbles. At equilibrium, ionic current is continuously flowing in the electrolyte while electrical current is flowing in the external circuit. The thickness of the oxide layer can be increased by choosing conditions that will make the oxidation rate higher than the dissolution rate, which will slowly increase the oxide layer thickness. This can be observed by noticing the current drop in the external circuit as the oxide thickness increases [18].

2.3.2 Mechanistic model of nanotube array formation

The key processes responsible for anodic formation of nanoporous alumina and titania [19-21] appear to be the same, and are fundamental to the formation of straight titania nanotubes. The key processes are: (1) Oxide growth at the surface of the metal occurs due to interaction of the metal with O^{2-} or OH^- ions [22]. After the formation of an initial oxide layer, these anions migrate through the oxide layer reaching the metal/oxide interface where they react with the metal. (2) Metal ion (Ti^{4+}) migration from the metal at the metal/oxide interface; Ti^{4+} cations will be

ejected from the metal/oxide interface under application of an electric field that move towards the oxide/electrolyte interface. (3) Field assisted dissolution of the oxide at the oxide/electrolyte interface [20-26]. Due to the applied electric field the Ti–O bond undergoes polarization and is weakened promoting dissolution of the metal cations. Ti^{4+} cations dissolve into the electrolyte, and the free O^{2-} anions migrate towards the metal/oxide interface, see process (1), to interact with the metal. (4) Chemical dissolution of the metal, or oxide, by the acidic electrolyte also takes place during anodization. Chemical dissolution of titania in the electrolyte plays a key role in the formation of nanotubes rather than a nanoporous structure. As the anodization process begins the initial oxide layer, formed due to interaction of the surface Ti^{4+} ions with oxygen ions (O^{2-}) in the electrolyte, is seen uniformly across the surface. The overall reactions for anodic oxidation of titanium can be represented as

$$2H_2O \rightarrow O_2 + 4e^- + 4H^+ \tag{2.1}$$

$$Ti + O_2 \rightarrow TiO_2 \tag{2.2}$$

In the initial stages of the anodization process field-assisted dissolution dominates chemical dissolution due to the relatively large electric field across the thin oxide layer [20,27]. Small pits formed due to the localized dissolution of the oxide, represented by the following reaction, act as pore forming centers:

$$TiO_2 + 6F^- + 4H^+ \rightarrow TiF_6^{2-} + 2H_2O \tag{2.3}$$

Then, these pits convert into bigger pores and the pore density increases. After that, the pores spread uniformly over the surface. The pore growth occurs due to the inward movement of the oxide layer at the pore bottom (barrier layer) due to processes (2.1)–(2.3). The Ti^{4+} ions migrating from the metal to the oxide/electrolyte interface dissolve in the electrolyte. The rate of oxide growth at the metal/oxide interface and the rate of oxide dissolution at the pore-bottom/electrolyte interface ultimately become equal, thereafter the thickness of the barrier layer remains unchanged although it moves further into the metal making the pore deeper. The thickness of the tubular structure ceases to increase when the chemical dissolution rate of the oxide at the mouth of the tube (top surface) becomes equal to the rate of inward

movement of the metal/oxide boundary at the base of the tube. Higher anodization voltages increase the oxidation and field-assisted dissolution hence a greater nanotube layer thickness can be achieved before equilibrating with the chemical dissolution.

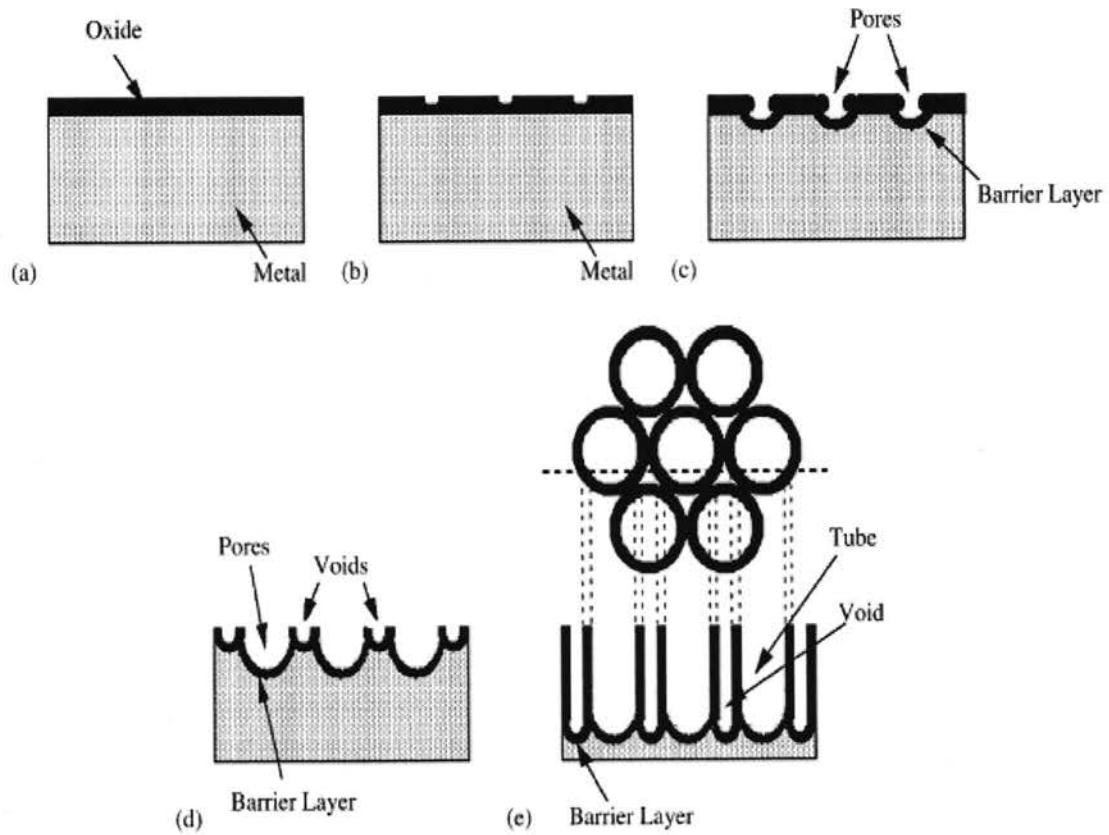

Figure 2.7 Schematic diagram of the evolution of a nanotube array at constant anodization voltage: (a) oxide layer formation, (b) pit formation on the oxide layer, (c) growth of the into scallop shaped pores, (d) metallic part between the pores undergoes oxidation and field assisted dissolution, and (e) fully developed nanotube array with a corresponding top view [22].

With the onset of anodization, a thin layer of oxide forms on the titanium surface shown in Figure 2.7a. Small pits originate in this oxide layer due to the localized dissolution of the oxide shown in Figure 2.7b making the barrier layer at the bottom of the pits relatively thin which, in turn, increases the electric field intensity across the remaining barrier layer resulting in further pore growth shown in Figure 2.7c. The pore entrance is not affected by electric field-assisted dissolution and hence

remains relatively narrow, while the electric field distribution in the curved bottom surface of the pore causes pore widening, as well as deepening of the pore. As the Ti–O bond energy is high (323 kJ/mol), in the case of titania it is reasonable to assume that only pores having thin walls can be formed due to the relatively low ion mobility and relatively high chemical solubility of the oxide in the electrolyte, hence un-anodized metallic portions can initially exist between the pores. As the pores become deeper the electric field in these protruded metallic regions increases enhancing the field-assisted oxide growth and oxide dissolution, hence simultaneously with the pores well-defined inter-pore voids start forming, as seen Figure 2.7d. Thereafter, both voids and tubes grow in equilibrium. The nanotube length increases until the electrochemical etch rate equals the chemical dissolution rate of the top surface of the nanotubes. After this point is reached the nanotube length will be independent of the anodization duration, as determined for a given electrolyte concentration and anodization potential [20, 28].

2.3.3 Influence of anodization voltage

At lower applied potential, the Ti surface consisted of oxide layer with random pits whereas, at higher applied potential, irregular structure was formed as the balance between the chemical dissolution and electric field dissolution, and oxidation process was interrupted. It can be concluded that the effective surface area and crystallization of TiO_2 nanotube arrays are important factors influencing the efficiency of photoelectrochemical performance [29]. Anodization time is a parameter of self-organized TiO_2NTs/Ti foils because it has three stages for self organization: 1) Forming barrier layer of titanium that interacts with electrolyte when voltage was applied 2) Oxide growth and dissolution are appear, 3) The balance of growth and chemical dissolution [30]. At that point, the TiO_2NTs/Ti foils were studied in glycerol/water/ammonium fluoride electrolytes at 20 volts and varied anodization time. The result was shows the different TiO_2 morphologies: at 0, 3, 10, 30, 60 min formed compact TiO_2 layer, initial growth, initial porous layer, remaining initial porous layer and order tubes and self-organized nanotubes layer, repectively, as seen in Figure 2.9. Then, anodization time could be optimized for self-organized TiO_2NTs/Ti foils.

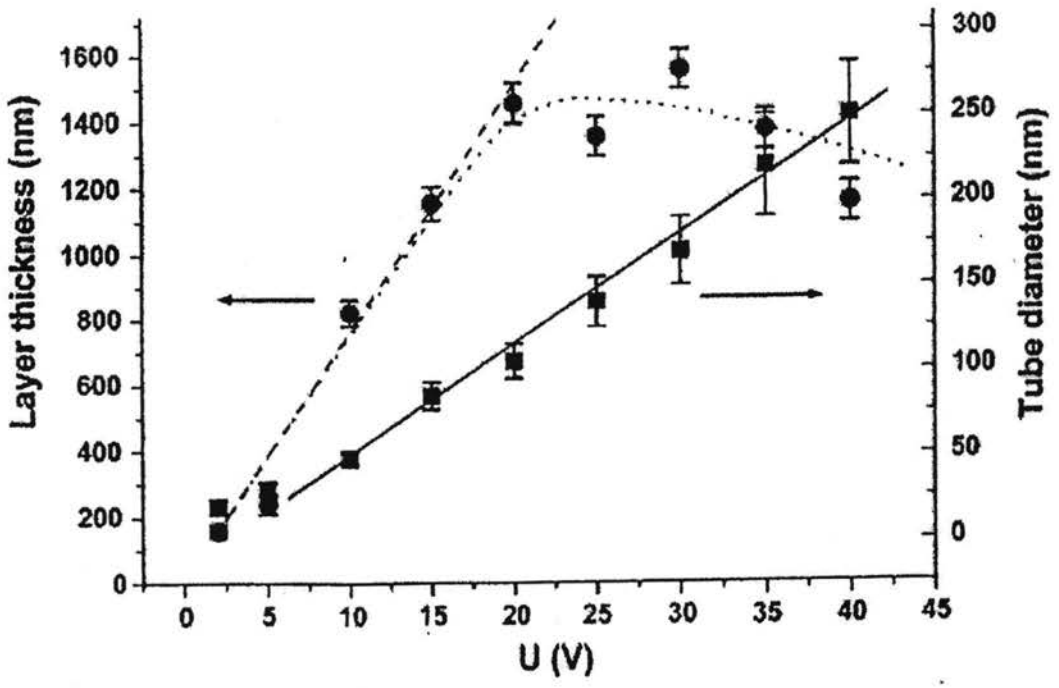

Figure 2.8 Tube diameter and thickness of the nanotube layers [30].

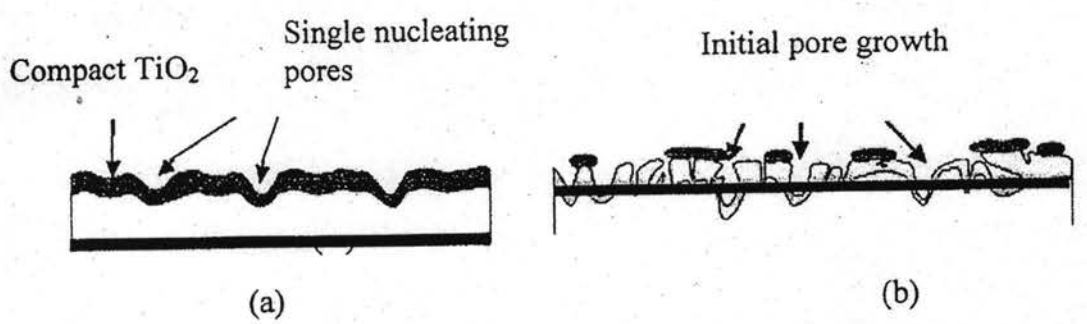

Figure 2.9 Schematic diagrams of different stages of the TiO_2 nanotube formation Anodization stopped after (a) 0 min, (b) 3 min from reaching 20 volts [31].

2.3.4 Influence of pH value

Nanotube arrays several microns in length have been fabricated using KF (or NaF with equivalent results) electrolytes of variable pH. Electrolyte pH affects both the behavior of the electrochemical etch and chemical dissolution owing to the hydrolysis of titanium ions. With increasing pH the hydrolysis content increases, which slows the rate of chemical dissolution. Longer nanotubes can be formed in

higher pH solutions that remain acidic. On increasing pH values the hydrolysis content increases, resulting in a significant amount of hydrous titanic oxide precipitated on the nanotube surface. Our studies showed that the best pH range for formation of relatively longer nanotubes is between pH 3 and 5; lower pH forms shorter but clean nanotubes, while higher pH values result in longer tubes that suffer from unwanted precipitates [32].

2.4 Dye-sensitized solar cell (DSSC)

Dye-sensitized solar cell (DSSC) is a real revolution in solar energy after 40 years of the invention of silicon solar cell [1, 2]. The working mechanism is based on photoelectrochemical mechanism, resembling the photosynthesis in plant leaves. The efficiencies of the DSSC is high as those obtained from amorphous silicon solar cells (10-11%). It was invented in 1991 by Prof Michael Graetzel in Switzerland. As the dye molecules are hit by light, electrons in the dye are transmitted to TiO_2. Then the electrons are collected by front electrode and supplied to external load. The dye molecules are then electrically reduced to their initial states by electrons transferred from redox couple in the electrolyte. The oxidized ions in the electrolyte, diffuse to the back electrode to receive electrons.

Major differences of DSSCs from other semiconductor solar cells are that the sunlight is not mainly absorbed by the semiconductor (TiO_2) and that the electron–hole pair is separated not by the built in potential of a p–n junction. A visible component of the solar light generates electron–hole pairs in the dye sensitizer which anchors on the photoanode of wide bandgap semiconductor nanoparticles. When the electron–hole pairs are formed in the dye molecules, they are quickly separated at a picosecond scale due to the difference in energy levels. Electrons are injected from the dye to the conduction band of the photoanode, and are transferred to the transparent conducting oxide (TCO) film that is coated on the glass. Holes in the dye molecules are delivered to the electrolyte through a redox reaction. In this structure, the maximum output voltage is the difference between Fermi energy of the semiconductor film and redox potential of the electrolyte [29].

2.5 Working principle of the dye-sensitized solar cell (DSSC)

Light absorption is performed by a monolayer of dye (D) adsorbed chemically at the semiconductor surface and excited by a photon of light (Eq. (2.4)). After having been excited (D*) by a photon of light, the dye-usually a transition metal complex whose molecular properties are specifically for the task is able to transfer an electron to the semiconductor (TiO_2) by the injection process (Eq. (2.5)). The efficiency of a DSSC in the process for energy conversion depends on the relative energy levels and the kinetics of electron transfer processes at the liquid junction of the sensitized semiconductor/electrolyte interface. For efficient operation of the cell, the rate of electron injection must be faster than the decay of the dye excited state. Also, the rate of rereduction of the oxidized sensitizer (dye cation) by the electron donor in the electrolyte (Eq. (2.7)) must be higher than the rate of back reaction of the injected electrons with the dye cation (Eq. (2.6)), as well as the rate of reaction of injected electrons with the electron acceptor in the electrolyte (Eq. (2.8)). Finally, the kinetics of the reaction at the counter electrode must also guarantee the fast regeneration of charge mediator (Eq. (2.8)), or this reaction could also become rate limiting in the overall cell performance [15-19].

$$D + h\upsilon \rightarrow D^* \tag{2.4}$$

$$D^* \rightarrow D^+ + e_{cb} \tag{2.5}$$

$$D^+ + e_{cb} \rightarrow D \tag{2.6}$$

$$D^+ + \frac{3}{2} I^- \rightarrow D + \frac{1}{2} I_3^- \tag{2.7}$$

$$\frac{1}{2} I_3^- + 2e_{(pt)} \rightarrow \frac{3}{2} I^- \quad , \quad I_3^- + 2e_{(cb)} \rightarrow 3I^- \tag{2.8}$$

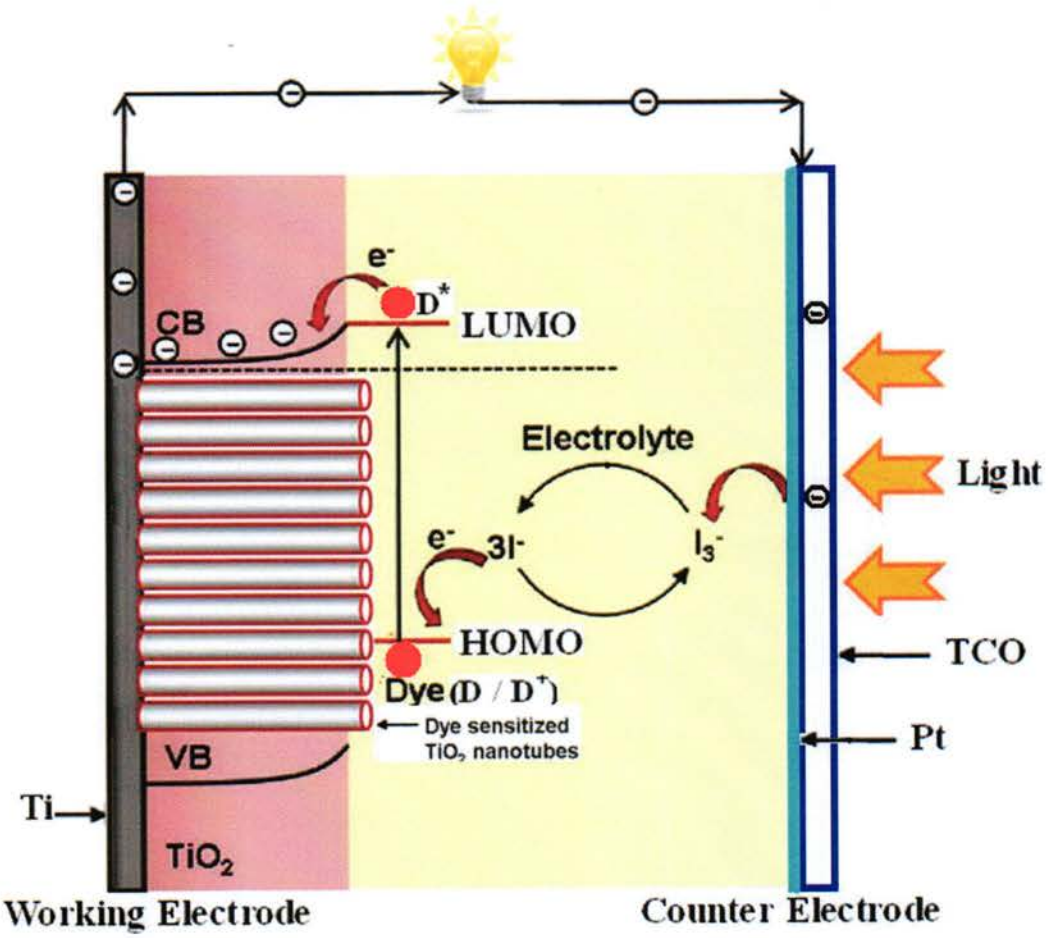

Figure 2.10 Schematic energy diagram and electron-hole transfer processes of DSSCs.

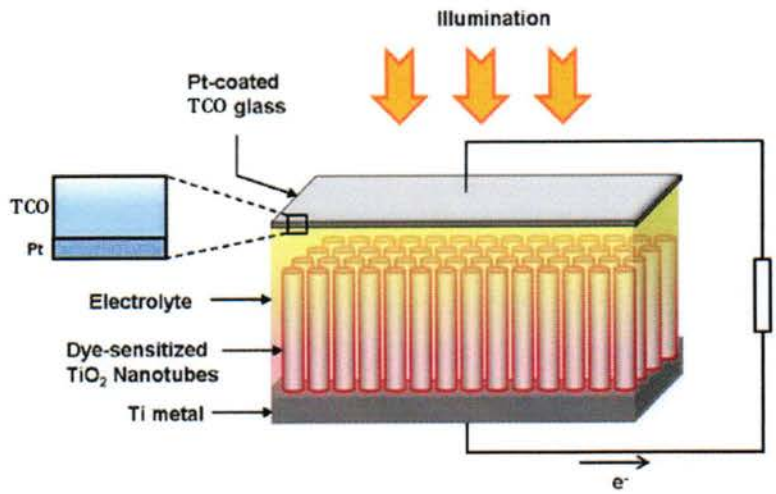

Figure 2.11 Schematic representation of typical solar cell construction using TiO_2 nanotubes grown on a Ti substrate [33].

2.6 The components of the dye-sensitized solar cell (DSSC)

2.6.1 Semiconductor photoanode

Semiconductors such as TiO_2, ZnO and SnO_2 have been under extensive investigation due to their wide application in energy storage and environmental remediation. They act as sensitizers to facilitate light-reduced redox processes because of their conductive electronic structure, referred to as valence band and conduction band. Band positions of several commonly used semiconductors are shown in Figure 2.11. In the quantum physics theory, a photon with energy ($h\nu$) that exceeds or matches the band gap (Eg) of a semiconductor can excite an electron to the conduction band leaving a hole with a positive charge at the valence band. These charges can either be transferred to the external circuit to provide electrical current or be utilized to catalyze a certain chemical reaction.

Titanium dioxide exits in three natural forms. Among them the most stable form is rutile, which is at the equilibrium phase for any temperature. Though rutile form is more stable, anatase is perceived to be more chemically active when used in dye-sensitized solar cells. Anatase is metastable and has a trend to convert to rutile upon heating. Hence, the phase constituents are greatly influenced by the synthesis processing method. In order to study this phase conversion influence, experiments were conducted to compare dye-sensitized rutile-and anatase-based TiO_2 solar cells [34]. Dye-sensitized solar cells (DSSCs) fabricated with rutile and anatase films at the same thickness were subjected to the simulated AM 1.5 solar illumination. Results show essentially the same value of open-circuit voltage (Voc), whereas the short-circuit photo current (Isc) of the anatase-based cell is 30% higher than that of rutile-based cell. The difference in short-circuit current is attributed to the lower amount of dye absorption by the rutile film, owing to a relatively smaller specific surface area. The electron transfer rate in rutile film is generally slow in nature due to the low coordination number associated with the particle packing density, which is identified by intensity- modulated photocurrent spectroscopy.

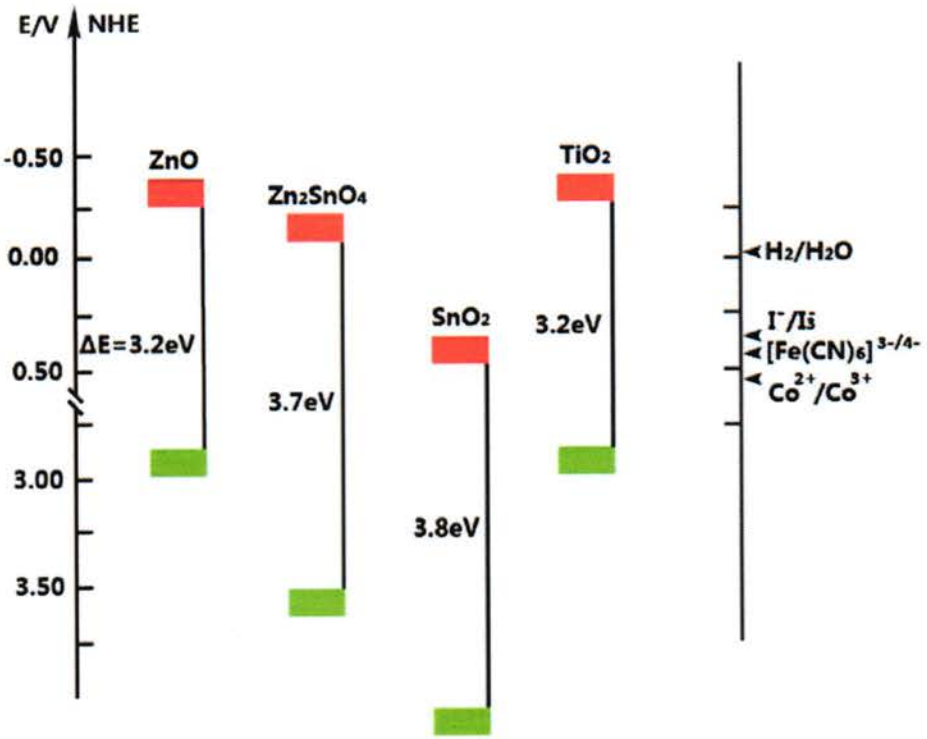

Figure 2.12 Band positions of several semiconductors and potentials of redox couples are represented using normal hydrogen electrode [33-34].

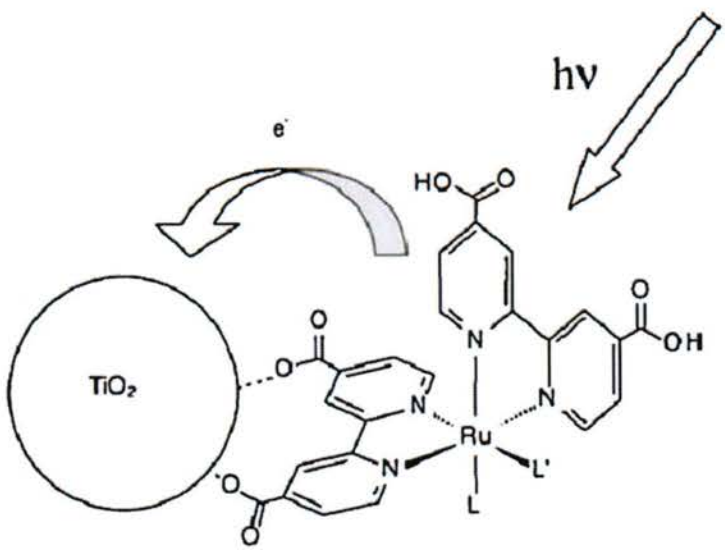

Figure 2.13 Absorption of dye molecule on TiO_2 via two of its four carboxylate groups [35].

2.6.2 Counter electrode

The prerequisite of a material used as counter electrode in DSSC is that it should have a low charge transfer resistance and high exchange current densities for the reduction of the oxidized form of the charge mediator [36]. The counter electrode serves to transfer electrons arriving from the external circuit back to the redox electrolyte. It also has to carry the photocurrent over the width of each solar cell. Hence, it must be well conducting and exhibit a low overvoltage for reduction of the redox couple. Till now, Pt has been the desired material for the counter electrode since it is an excellent catalyst for I_3^- reduction.

An interesting low cost alternative for Pt is carbon (C), because it combines sufficient conductivity and heat resistance as well as corrosion resistance and electrocatalytic activity for the I_3^- reduction. Porous C electrodes are easily prepared from graphite powder, which consists of plate like crystals that, on deposition from a liquid dispersion and drying, will preferentially align in the plane of the counter electrodes, resulting in a high conductivity in this plane. Pt/C black electrode showed the same efficiency and lower cost compared with Pt electrode alone [37-39].

2.6.3 Electrolyte

One of the most important DSSC components is the dye sensitizer, which represents the photodriven elctron pump of the device. It allows an independent electron injection into the semiconductor conduction band and conversion of visible and near infrared photons to electricity. Several organic and inorganic compounds have been investigated for semiconductor sensitization, such as chlorophyll derivatives [39], porphyrins [40], phtalocyanines [41-42], platinum complexes [43-44], fluorescent dyes [45], carboxylated derivatives of anthracene [46], polymeric films [47], and coupled semiconductors with lower-energy bandgaps [48], among others.

The electrolyte is a key component of all dye-sensitized solar cells (DSSC). It functions as charge carriers collecting electrons at the cathode and transporting the electrons back to the dye molecule. In terms of the cell efficiency, the most popularly used electrolyte is the iodide/triiodide (I^-/I_3^-) redox couple in an organic matrix, generally acetonitrile. However, there exist undesirable intrinsic properties which are inherent of a liquid electrolyte significantly affecting a device's

long-term durability and operational stability. For example, not only the leakage of toxic organic solvent will cause environmental contamination, but also the evaporation of volatile iodine ions will increase the overall internal resistance by lowering concentration of the charge carrier. To overcome these disadvantages, research has been conducted to develop non-traditional electrolytes, quasi-solid state and solid state electrolytes [21].

The electrolyte is a neutral sink of I^- and I_3^- feeding the reactions at the electrodes and maintaining the redox potential in the bulk of the electrolyte via the fast redox reaction of the I^-/I_3^- pair. This redox reaction in the electrolyte is a two electron reaction [49]:

$$3I^- \rightarrow I_3^- + 2e^- \tag{2.9}$$

which is composed of a series of successive reactions:

$$(I^- \rightarrow I + e^-) \times 2 \quad \text{charge transfer reaction} \tag{2.10}$$

$$2I \rightarrow I_2 \quad \text{fast chemical reaction} \tag{2.11}$$

$$I_2 + I^- \rightarrow I_3^- \quad \text{fast chemical reaction} \tag{2.12}$$

Room temperature ionic liquid has good chemical and thermal stability, negligible vapor pressure, non flammability and high ionic conductivity. When incorporated into DSSCs, they serve both as a source of iodide and the solvent itself. Liquid electrolyte based organic solvent usually have high ionic conductivity and excellent interfacial contact property however there still exist problems such as leakage and volatility of the solvent which affect the long term performance of DSSCs [49,50]. A disadvantage of liquid electrolyte is that it may limit device stability because the liquid may evaporate when the cell is imperfectly sealed. Penetration of water or oxygen molecules and their reaction with the electrolyte may also worsen cell performance. Liquid electrolytes also make the construction of multi-cell modules difficult because cells must be connected electrically yet separated chemically, preferably on a single substrate. Among all of the solid-state cells, the one containing a p-type semiconductor possessed the advantage of easy preparation and higher stability

while the cells employing polymer electrolytes showed higher efficiency and wider practical future use with the proper encapsulation[51]. Based on their physical state, the electrolytes can be classified into 3 groups - liquid electrolyte, quasi-solid electrolyte and solid electrolyte [52].

2.6.4 Sensitizing materials

In DSSCs, the electronic excitation in the dye achieved through light absorption promotes dye molecule into a high energy state associated with the Lowest Unoccupied Molecular Orbital (LUMO). This simultaneously creates an electron deficiency in the low energy state - the Highest Occupied Molecular Orbital (HOMO). Electrons in the LUMO and HOMO states are separated by a difference in enthalpy (h) [48, 53].

$$\Delta h = \Delta E = E_{LUMO} - E_{Homo} \tag{2.13}$$

where, Δh = change in enthalpy,

ΔE = difference in energy,

E_{LUMO} = energy of the least unoccupied molecular orbital

E_{Homo} = energy of the highest occupied molecular orbital

The sensitizer plays a critical role in generating electron–hole pairs. Sensitizers for DSSCs need to satisfy following requirements:

(1) Energy levels of the sensitizers match well with those of oxide the semiconductors and electrolyte. In dye sensitizers, for example, LUMO of dye needs to be higher than the edge of the semiconductor conduction band for the electron injection, and HOMO of dye needs to be aligned with the redox potential of the electrolyte for the regeneration of the oxidized dye.

(2) Sensitizing materials are strongly anchored on the surface of the semiconductor film to decrease an interface resistance and to secure the stable bonding for a long time.

(3) Electrons in the sensitizing materials are quickly separated from counterpart holes and injected to the photoanodes before being recombined.

(4) Light absorption spectrum of the sensitizing materials ranges from UV region to near IR region, with an absorption peak at visible region. The optimum absorption peak position of the sensitizing material for a single junction of solar light is 920 nm.

(5) The sensitizing materials last for more than 20 years, which is equivalent to 100 million times turnovers of the sensitizing materials under sunlight.

Sensitizing materials compatible with DSSC type solar cells, are group into metal-complex dye, metal-free organic dye, natural dye, and quantum dots. Several types of the dye in DSSCs are reviewed in this section. A brief summary of high efficient dyes is listed in Table 2.2.

Table 2.2 Efficiencies of DSSCs using different dye sensitizer [29].

Dye	Efficiency of DSSCs
N3	11.03%
N719	11.18%
Black dye	11.10%
Z910	10.20%
K77	9.00%
D205	7.20%
C219	10.30%

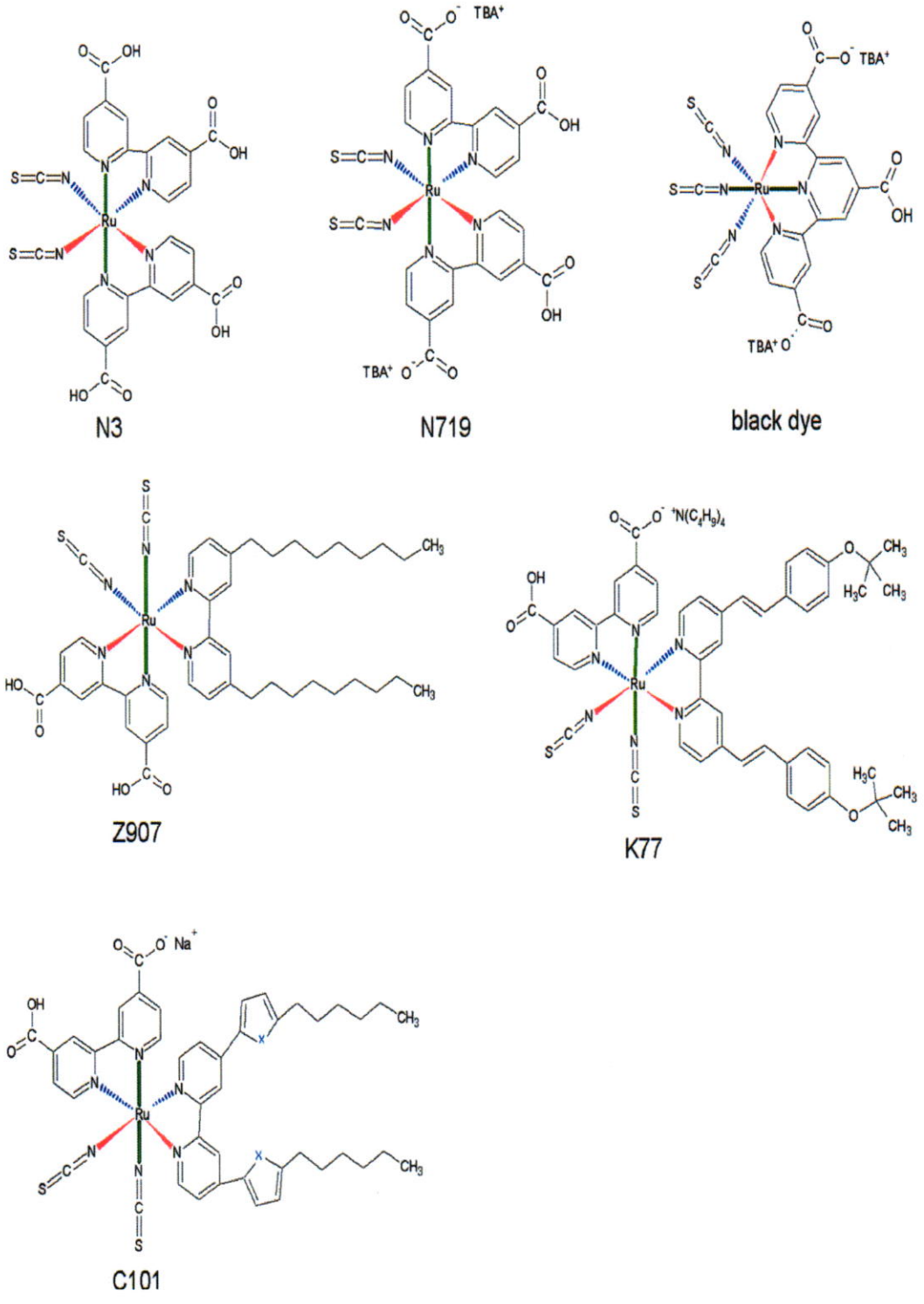

Figure 2.14 Structures of typical ruthenium-complex dye [29].

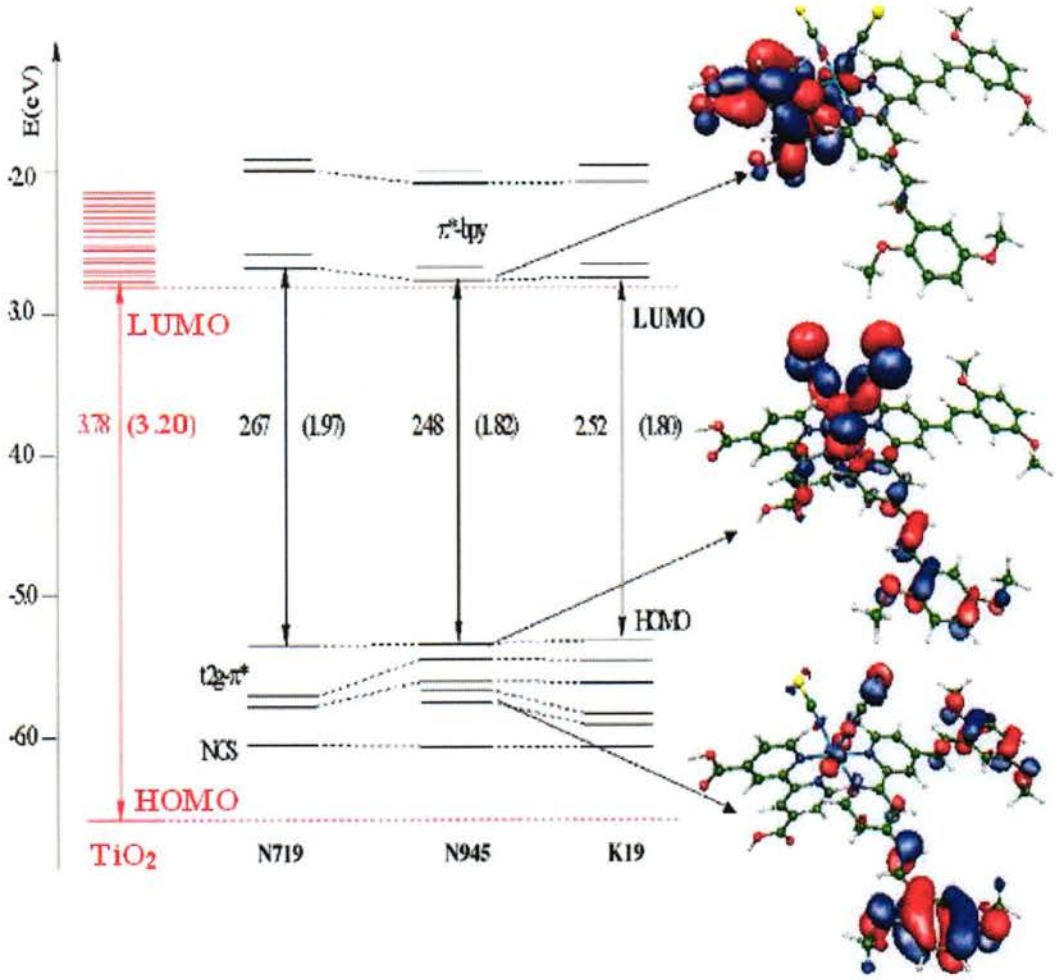

Figure 2.15 Molecular orbital energy diagram of N719, N945 and K19 compared to that of a TiO_2 nanoparticle mode [54].

2.7 Recombination

Recombination of the generated electrons with holes in the dye-sensitized nanostructured TiO_2 electrode can occur in principle after the electron injection or during its migration in the TiO_2 electrode on its way to the electrical back contact. Illumination of the dye-sensitized electrode initially in equilibrium (in the dark) generates a transient electric field between the injected electrons in the TiO_2 and the oxidized species in the electrolyte. This electric field could oppose in principle further charge separation and promote recombination. However, in the dye-sensitized solar cell the mobile ions in the electrolyte can easily rearrange and effectively screen the

light induced opposing fields in steady state conditions through out the electrode film, and thus enable an efficient charge separation. In the silicon solar cells, the recombination of charge carriers in trap states in surfaces, grain boundaries, and in the bulk degrades the cell performance easily, and thus semiconductor material of high crystal purity is required. In the dye-sensitized TiO_2 electrode, there is on the contrary vast amount of particle boundaries and a huge surface to volume ratio. Yet the dye solar cell does not seem to suffer from the recombination losses at the grain boundaries at all. The reason for this is that only electrons are transported through the semiconductor particles, while holes (oxidized ions) are carried by the electrolyte [55].

2.8 Measurements

The photovoltaic tests of quasi-solid-state dye-sensitized solar cells are carried out by measuring the J–V character curves under irradiation of white light from a AM 1.5. The photoelectronic performances [fill factor (FF) and overall energy conversion efficiency (η)] were calculated by the following equations [33-35, 56-57]:

$$FF = \frac{V_{\max} \times J_{\max}}{V_{oc} \times J_{sc}} \tag{2.14}$$

$$\eta = \frac{V_{\max} \times J_{\max}}{P_{in}} \times 100\% = \frac{V_{oc} \times J_{sc} \times FF}{P_{in}} \times 100\% \tag{2.15}$$

where FF is the fill factor
V_{oc} is the open-circuit voltage
$V_{\max}$ is the maximum voltage
J_{sc} is the short circuit current density
$J_{\max}$ is the maximum current density
$P_{\max}$ is the maximum power
P_{light} is the incident light power
η is the energy conversion efficiency

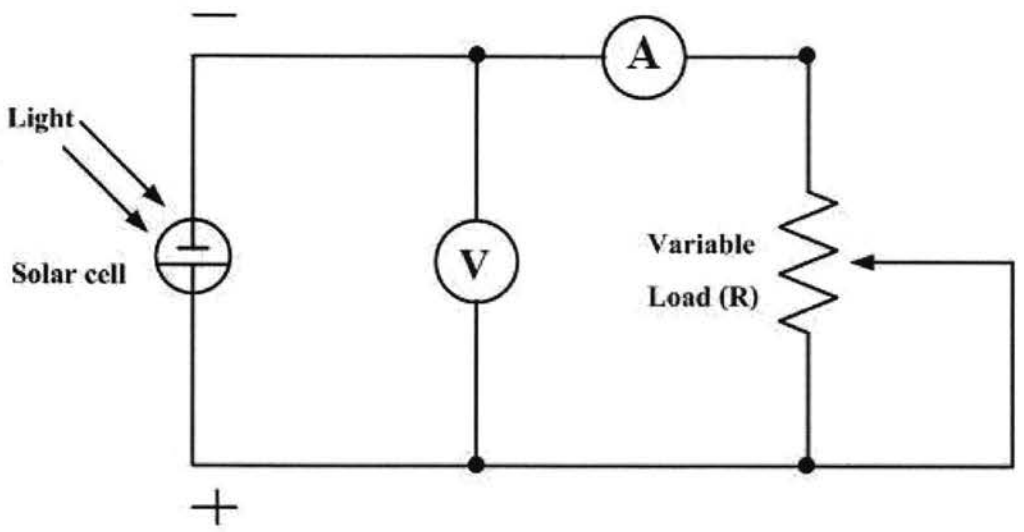

Figure 2.16 Light detector or solar cell I-V characteristic measurement set up [58-59].

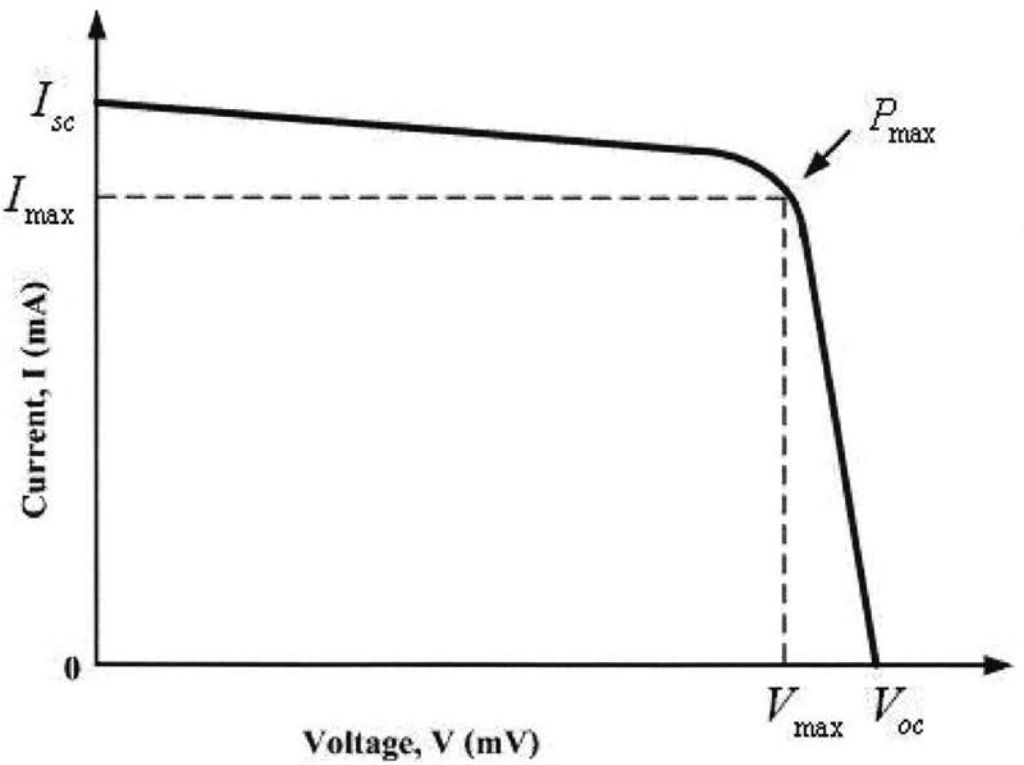

Figure 2.17 I-V characteristic curve of dye solar cell [36, 45].

2.9 Literature Review

TiO_2 nanotubes were produced by anodic oxidation by controlling the pH value of the electrolyte. In the strongly acidic electrolyte, the fast chemical dissolution rate restricts the growth of the TiO_2 nanotubes, while in the weakly acidic electrolyte the slow chemical dissolution rate accelerates the growth of the nanotubular TiO_2 layer. At first, a thick oxide layer was observed and then, round-shaped holes were randomly observed due to the F^- ions attacking the titanium oxide layer and then, stable equilibrium states were finally maintained. Furthermore, an investigation was conduced to understand why the TiO_2 nanotubes show a rough surface morphology and irregular wall thickness, which concluded that this resulted from the separation of the swollen pores [60].

Titania (TiO_2) nanotubes were prepared by anodizing titanium (Ti) foils in an electrochemical bath consisting of 1 M glycerol with 0.5 wt% NH_4F. The pH of the bath was kept constant at 6 and the anodization voltage was varied from 5 V, 20 V to 30 V. It is found that the morphology of the anodized titanium is a function of anodization voltage with pits-like oxide formed for the sample made at 5 V and samples made at 20 V and 30 V consisted of well-aligned nanotubes growing perpendicularly on the titanium foil. However, the nanotubes formed on the samples made at 30 V were not uniform in terms of the nanotubes' diameter and wall thickness. Regardless of the anodization voltage, as anodised samples were amorphous [61].

TiO_2 nanotube arrays were prepared by anodic oxidation in an NH_4F/H_3PO_4 electrolyte. Various anodization conditions, including magnetic stirring rate, F- concentration, voltage and time, can be varied to obtain TiO_2 nanotube arrays with a uniform and well-ordered morphology. The results show that stirring rate, F- concentration and voltage have important effects on the morphology and pore diameter, whereas anodization time affects the length of the TiO_2 nanotube arrays. Higher anodic voltage leads to larger pore diameter and greater anodization time yields longer tubes, which can adsorb more dye [6].

TiO_2 nanotube arrays were grown on conductive Ti substrates by anodization in glycerol electrolyte. The TiO_2 nanotubes were vertically grown, and adhered perfectly to the substrates. The diameter of the nanotube was gradually

increased with the increase anodizing voltage, at the same time, the surface area of nanotube attached with dye molecules more. When the illumination was from the backside, the incident light passing though the counter electrode can preferable enter into the larger pore-size nanotubes [62].

Anodic titanium oxide (ATO) was fabricated by anodization method of the Ti foil in an ethylene glycol electrolyte containing 0.38 wt% of NH_4F and 1.79 wt% of H_2O. Anodizing was carried out at the constant cell potential ranging from 30 to 70V at the temperature of 20 $^{\circ}$C. The thickness and aspect ratio of porous TiO_2 increase linearly with increasing anodizing potential [63].

Arrays of TiO_2 nanotubes were fabricated by the anodization of Ti foils and then used in assembling dyesensitized solar cells (DSSCs). TiO_2 nanotube arrays are used as photoanode for the application in dye-sensitized solar cell and the photovoltaic performance of 1.91% is achieved with a TiO_2 nanotube sample of 2.2 μm in length combining with N719 dye, and the corresponding photovoltaic parameters of 3.6 mA cm^{-2} in short circuit photocurrent density, 840 mV in open circuit potential, and 63.2% in fill factor [9].

CHAPTER 3
EXPERIMENTAL PROCEDURES

3.1 Materials and thin films preparation

Titanium Dioxide (TiO_2) nanotubes were synthesized by anodization method. The anodization conditions include the effect of pH values and anodization voltages. TiO_2 nanotube photoanodes have been synthesized on titanium foils by anodization method in the mixtures of ammonium fluoride (NH_4F), sodium hydroxide (NaOH) and sodium sulphate (Na_2SO_4) for the condition of different pH values. Then, we are interested in fabricating TiO_2 nanotubes by anodization method. The nanotubular layer was obtained by Ti metal anodization in an electrolyte consisting of a mixture of ethylene glycol ($C_2H_6O_2$), ammonium fluoride (NH_4F), and DI water under the applied voltages between 40, 50, 60 and 70 V for the condition of different voltages. The post anodization process was carried out by annealing in air at 450°C for 2 hrs. The characterization of TiO_2 nanotubes films is used by X-ray diffraction (XRD), scanning electron microscopy (SEM), and UV-vis spectrometer. In application, we test dye-sensitized solar cell by using TiO_2 nanotubes form anodization voltage condition as a working electrode.

3.2 Anodization method

In each fabrication, a Ti sheet, 0.25 mm in thickness and 99.7% in purity, was anodized at room temperature in ethylene glycol ($C_2H_6O_2$) that also contained 0.25% NH_4F (in mass) and 0.6% H_2O (in volume). Before the anodization, the sheet was cleaned ultrasonically in turn in isopropanol, de-ionized water and ethanol. A DC power source was used to drive the reaction. The Ti sheet was bound to the electrolytic cell via an O-ring and a Cu plate. One side of the sheet was in contact with the electrolyte and the opposite side, covered by a Cu plate, was connected to the power source with a conducting wire. The counter electrode was a piece of platinum (Figure3.1). The spacing between the two electrodes was approximately 5 cm. The anodization voltages were varied between 40, 50, 60 and 70 V and the Ti sheet were

subjected to a constant 5 hrs anodic time. Samples were washed with ultrasonic treatment to remove occluded ions from the surface of the TiO_2 nanotubes after anodization. All substrates were annealed at 450 °C for 2 hrs to obtain anatase crystalline phases of TiO_2 [20]. To investigate the surface morphology and microstructure of TiO_2NTs, all samples were characterized by SEM and XRD techniques.

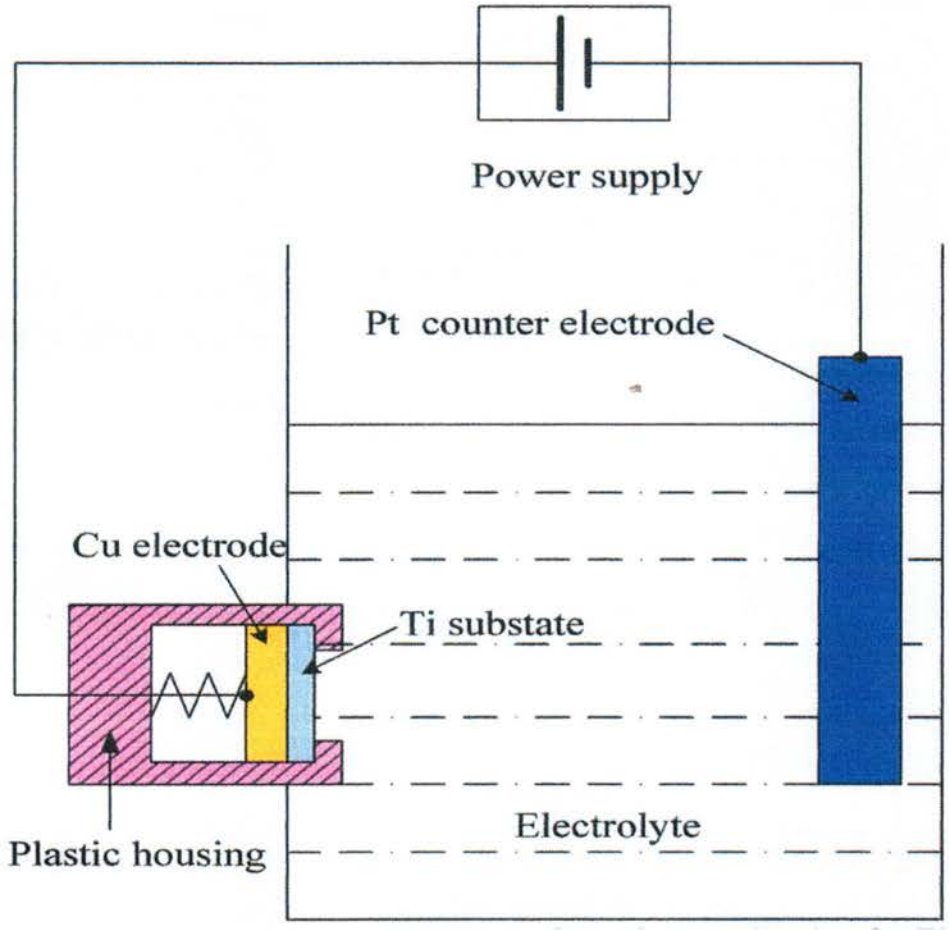

Figure 3.1 Experimental equipment diagram of anodization method for TiO_2NTs.

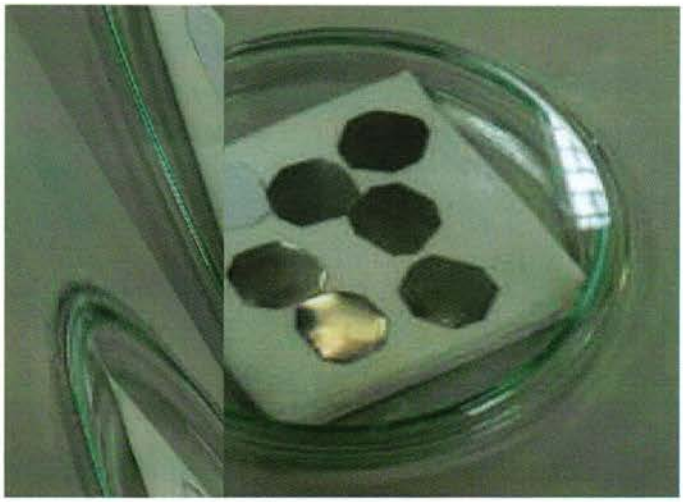

Figure 3.2 Ti foils before anodization process.

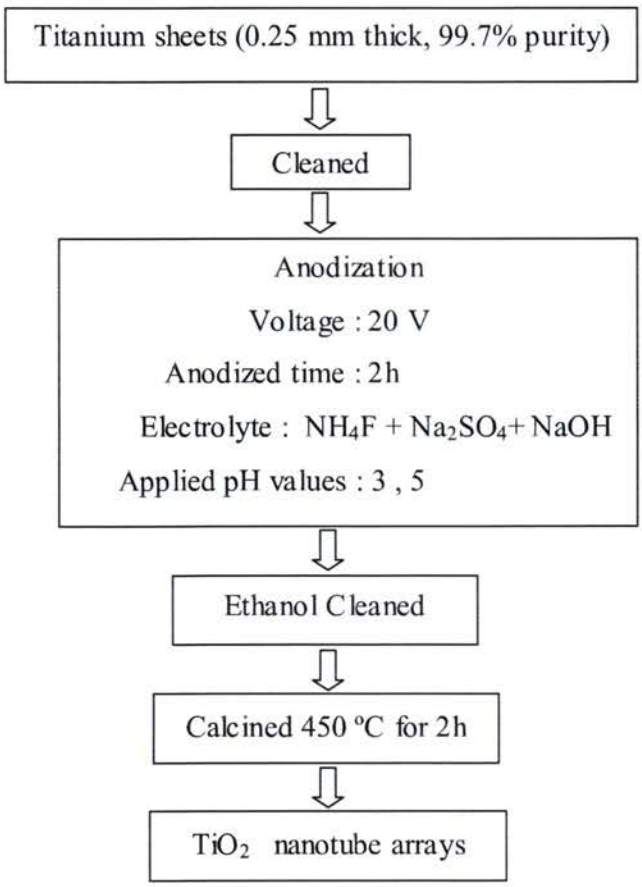

Figure 3.3 Schematic illustration of the preparation of TiO_2 nanotube arrays by anodization method for the condition of different pH values.

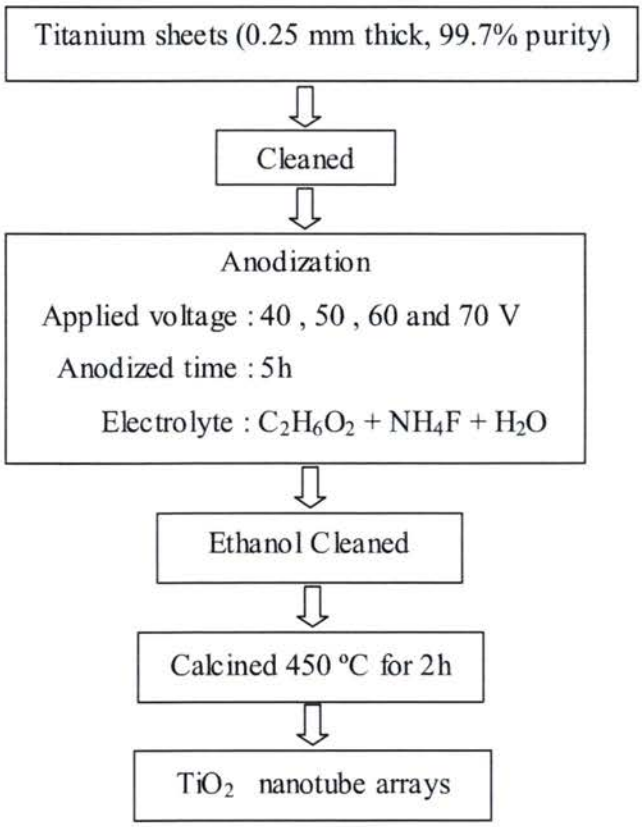

Figure 3.4 Schematic illustration of the preparation of TiO_2 nanotube arrays by anodization method for the condition of different voltages.

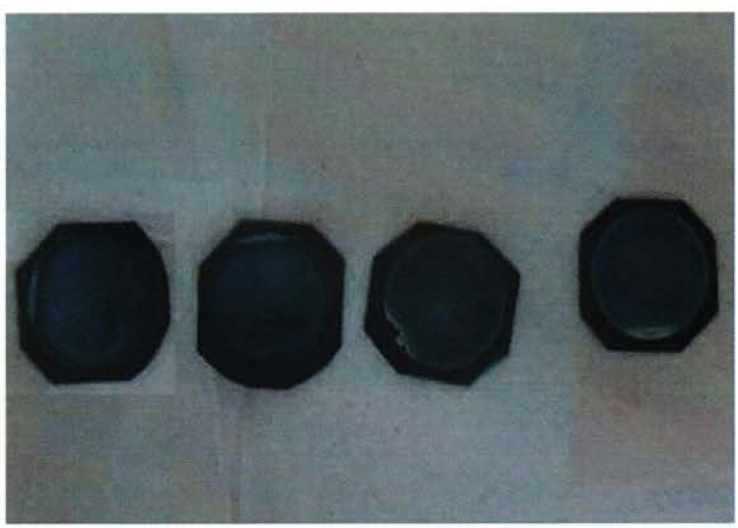

Figure 3.5 TiO_2 nanotube arrays after anodization process.

TiO_2 nanotube film was immersed in a dye solution (N719) for 24 hrs to absorb the dye adequately, then the dye sensitized TiO_2 film was washed up with anhydrous ethanol and dried in moisture-free air [29, 33, 56].

Figure 3.6 TiO_2 nanotube films were immersed in a dye solution (N719).

3.3 Electrolyte

An electrolyte was prepared as following. 0.6 M potassium iodide (KI) and 0.05 M iodine were mixed with solvent of ethylene carbonate (EC) and propylene carbonate (PC) (6:4, w/w) under stirring to form a homogeneous liquid electrolyte solution.

3.4 Dye-sensitized solar cell

To fabricate a dye-sensitized solar cell, the polymer gel electrolyte was injected into the aperture between a dye-sensitized TiO_2 nanotube film electrode (working electrode) and a platinized conducting glass sheet applied by electroplating (counter electrode). Then, the two electrodes were clipped together and epoxy resins were used as sealants [22].

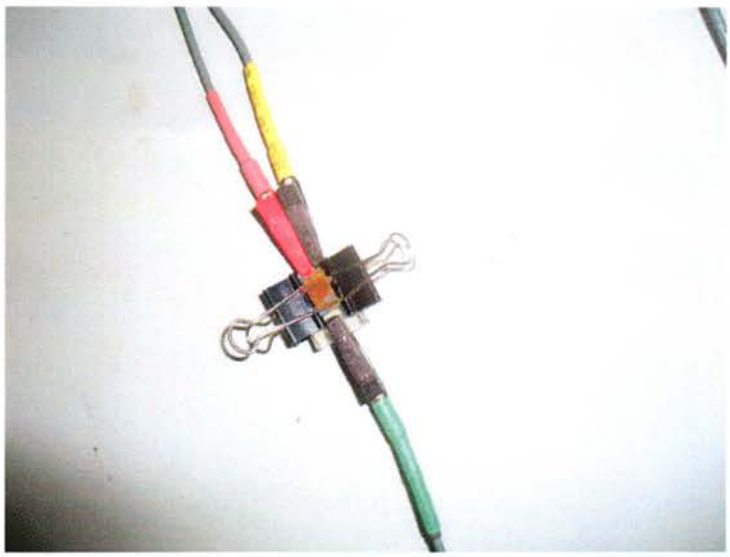

Figure 3.7 dye sensitized solar cell.

3.5 Measurement

The photovoltaic tests of dye-sensitized solar cells were carried out by measuring the J–V character curves under irradiation of 60 mW/cm^2 and the active cell areas were 0.25 cm^2. The photoelectronic performances [fill factor (FF) and overall energy conversion efficiency (η)] were calculated by the following equations [33-34, 56, 57]:

$$FF = \frac{V_{\max} \times J_{\max}}{V_{oc} \times J_{sc}} \tag{3.1}$$

$$\eta = \frac{V_{\max} \times J_{\max}}{P_{in}} \times 100\% = \frac{V_{oc} \times J_{sc} \times FF}{P_{in}} \times 100\% \tag{3.2}$$

where FF is the fill factor
V_{oc} is the open-circuit voltage
$V_{\max}$ is the maximum voltage
J_{sc} is the short circuit current density
$J_{\max}$ is the maximum current density
$P_{\max}$ is the maximum power
P_{light} is the incident light power
η is the energy conversion efficiency

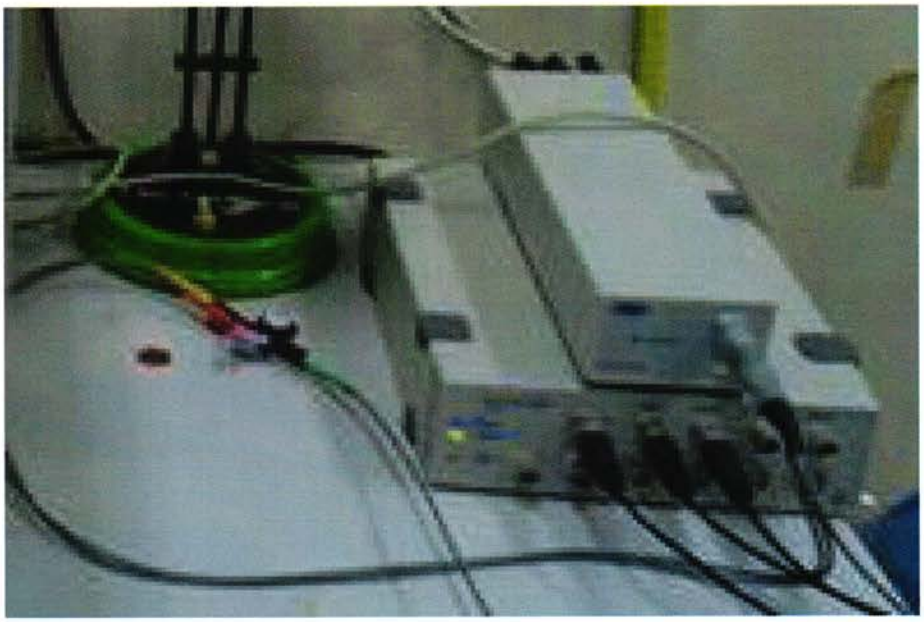

Figure 3.8 measurement of dye sensitized solar cell by Potentiostate.

3.6 Scope of fabrication of dye sensitized solar cells

We are interested in fabricating TiO_2 nanotubes by anodization method. The nanotubular layer was obtained by Ti metal anodization in an electrolyte consisting of a mixture of ethylene glycol ($C_2H_6O_2$), NH_4F, and DI water under the applied voltages between 40, 50, 60 and 70 V. The characterization of TiO_2 nanotubes films is used by X-ray diffraction (XRD), scanning electron microscopy (SEM), and UV-vis spectrometer. In application, we show dye-sensitized solar cell by using TiO_2 nanotubes as a working electrode.

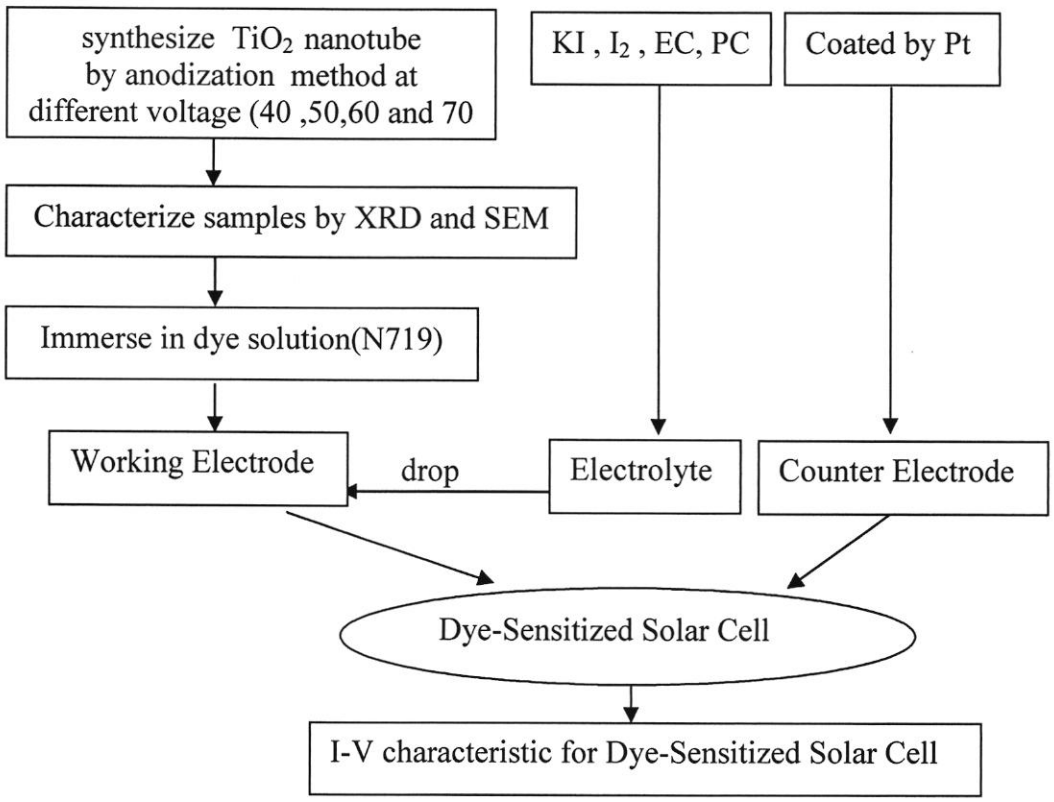

Figure 3.9 Scope of fabrication of dye-sensitized solar cell.

CHAPTER 4
RESULTS AND DISCUSSION

4.1 Effect of pH values

Figure 4.1 shows XRD patterns of Ti sheet post annealed TiO_2 nanotubes. The XRD patterns show that the phases of TiO_2 nanotubes are anatase. The anatase (101) peak shows prominently when the anodization was carried out in the electrolyte with pH 3. The SEM image of post-annealed TiO_2 nanotubes grows in the different pH electrolytes. The morphology of the TiO_2 was found to be influenced by pH of the anodizing electrolyte. The prepared sample with the anodization in pH 5 electolyte was the titania films with anatase phase. The TiO_2 nanotubes were not observed while the samples with anodization in pH 3 electrolyte showed clearly titania nanotubes with diameters of about 100 nm as shown in Figure 4.3.

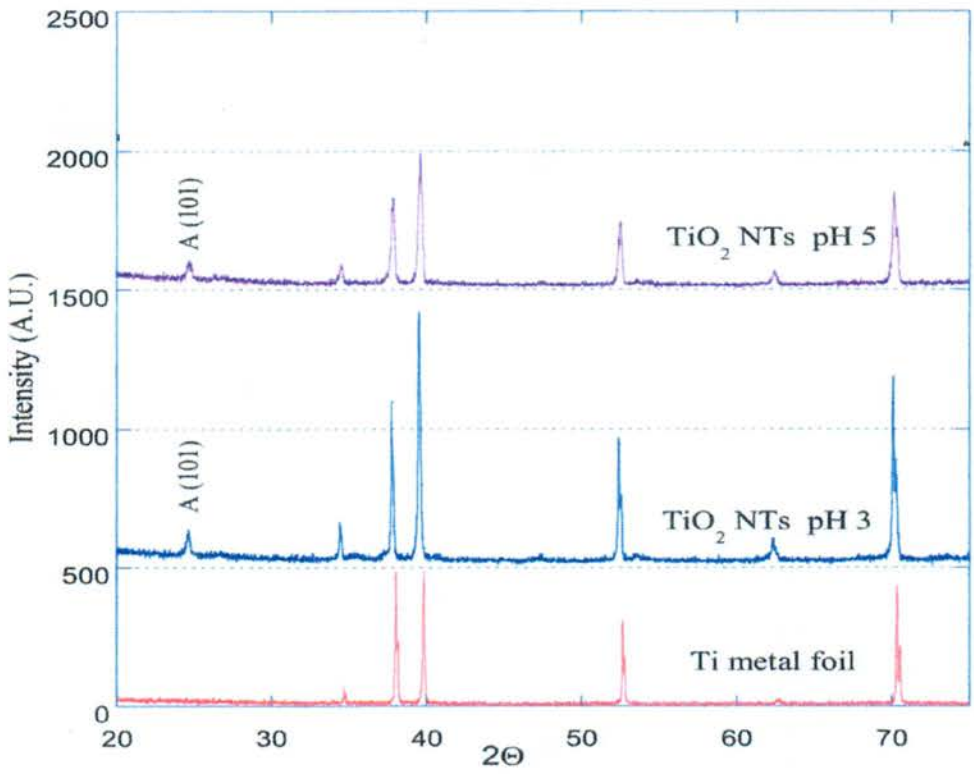

Figure 4.1 XRD patterns of TiO_2 NTs and in TiO_2/Ti foil; pH 5 and pH 3.

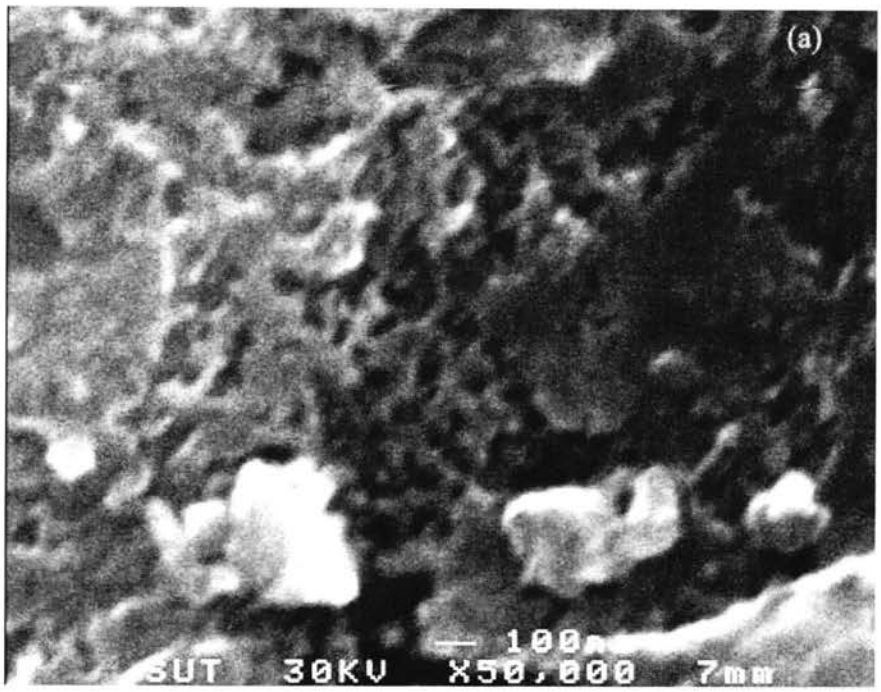

Figure 4.2 SEM image, the top view of TiO_2 NTs/Ti foil as formed in mixed electrolyte at pH 5.

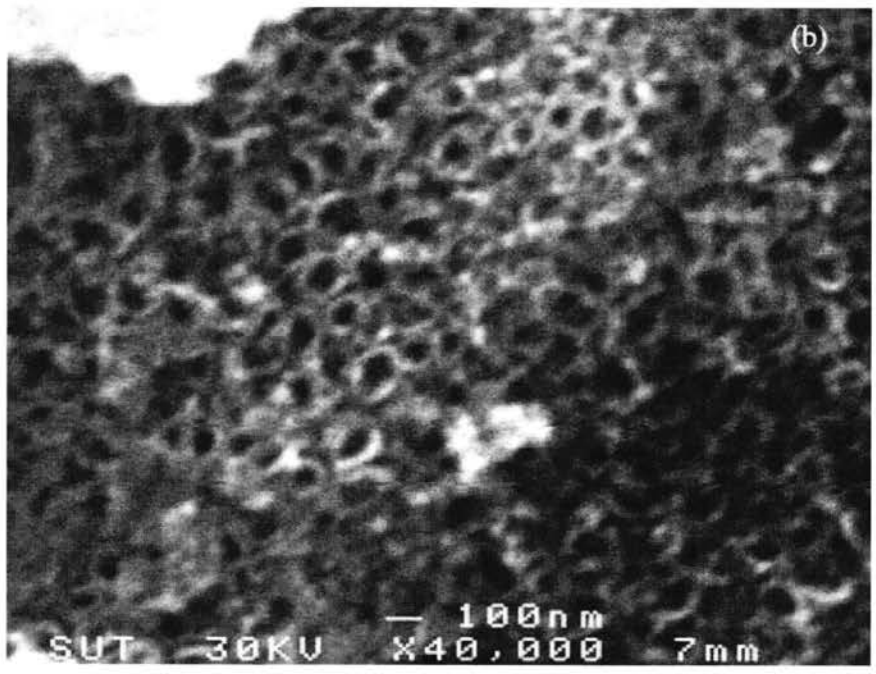

Figure 4.3 SEM image, the top view of TiO_2 NTs/Ti foil as formed in mixed electrolyte at pH 3.

4.2 Effect of anodization voltages

Figure 4.4 shows XRD diffraction patterns of nanotube films as prepared and calcined at 450 °C for 2 hrs which the TiO_2 nanotubes were fabricated in different voltages (40, 50, 60 and 70 V). The XRD diffraction patterns of nanotube films as prepared TiO_2 nanotube arrays are amorphous after anodization. As the TiO_2 nanotubes have been calcined they possess polycrystalline nature. This is confirmed by XRD analysis. The presence of peak in XRD pattern indicates that the calcined nanotubes are composed of pure anatase phase at all different applied voltages. Good crystallinity is required for smooth electron flow in the nanotubes for the efficient dye-sensitized solar cells [64].

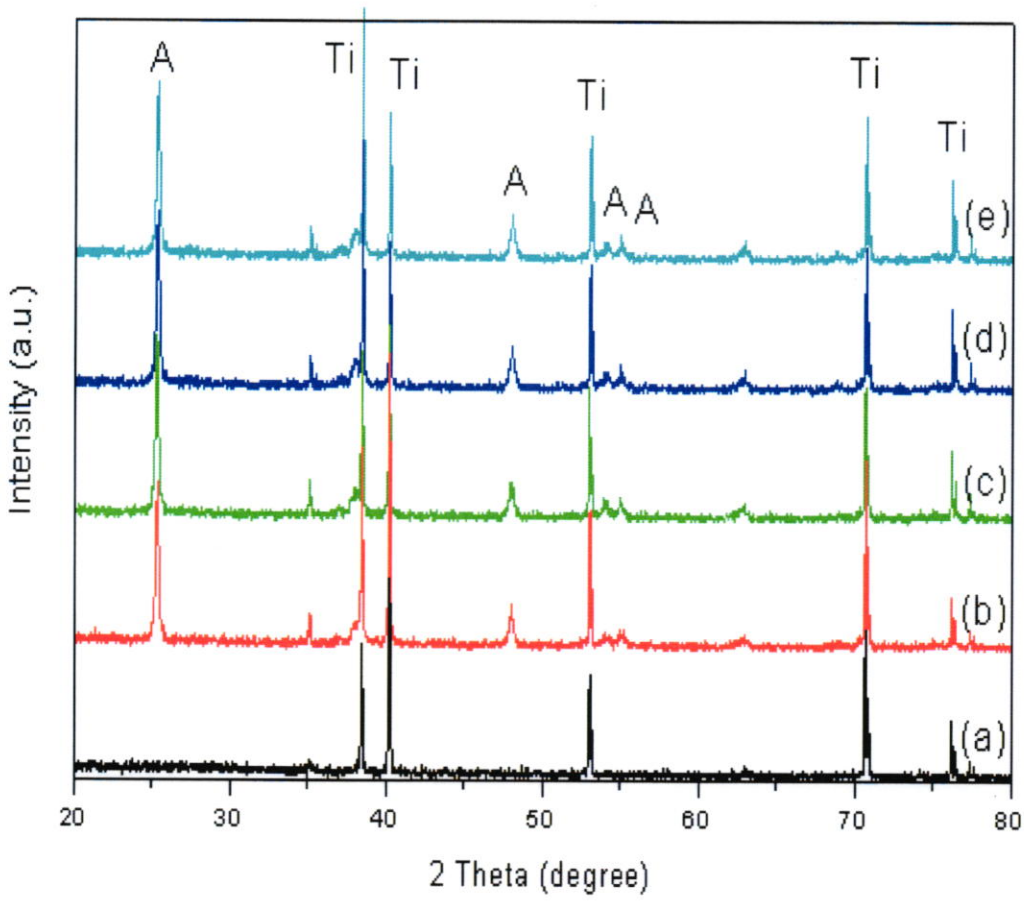

Figure 4.4 XRD patterns of (a) before annealing and after annealing at different voltages at 450 °C for 2 hrs : (b) 40 V, (c) 50 V, (d) 60 V and (e) 70 V.

Figure (4.5-4.8) shows the SEM micrographs of TiO_2 nanotubes obtained by anodization for 5 hours in 25% NH_4F + $C_2H_6O_2$ + 0.6% H_2O aqueous solution at room temperature at different voltages (40, 50, 60 and 70 V, respectively) the calcinated at 450 °C for 2 hours. Anodization voltage strongly affects the spacing and pore size of TiO_2 nanotubes because the electrochemical etching rate depends on the anodization potential. The nanotube formation process includes electrochemical etching of Ti and chemical dissolution of oxide formed. The nanotube depth increases till the electrochemical etching rate becomes equal to the chemical dissolution of the top surface of the nanotubes. Higher anodization voltages increase the oxidation and field assisted dissolution hence a greater nanotube layer thickness can be formed before equilibrating with the chemical dissolution.

In order to evaluate the influence of the applied voltage on the average diameter of TiO_2 nanotubes, anodization experiments at different applied voltages have been performed. The key factor controlling the tube diameter is the anodization voltage [62]. The higher applied voltage can strike out bigger pits, which act as pore forming centers. It was obvious that the average diameter of the nanotubes was proportional to the applied potential. The average pore diameter of the nanotubes formed at 40, 50, 60 and 70V were approximately 90, 125, 150 and 200 nm, respectively. It is clearly shown that the nanotube diameter increases with the higher anodization voltage [45-46]. The corresponding average pore diameter of TiO_2 nanotubes as a function of the anodization voltage is reported.

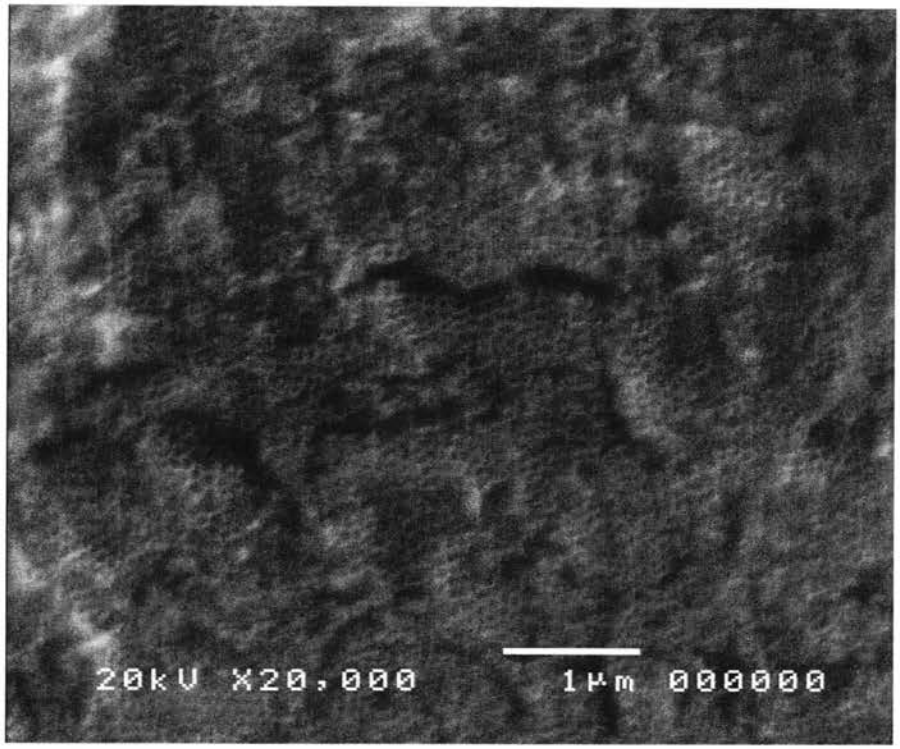

Figure 4.5 SEM image of TiO_2 nanotube arrays at 40 V.

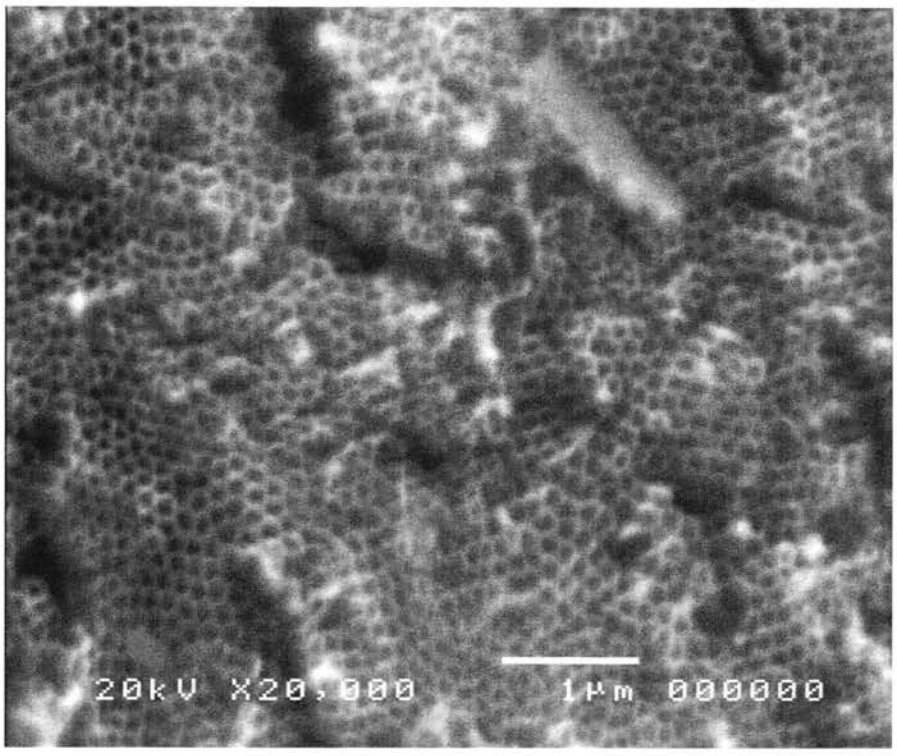

Figure 4.6 SEM image of TiO_2 nanotube arrays at 50 V.

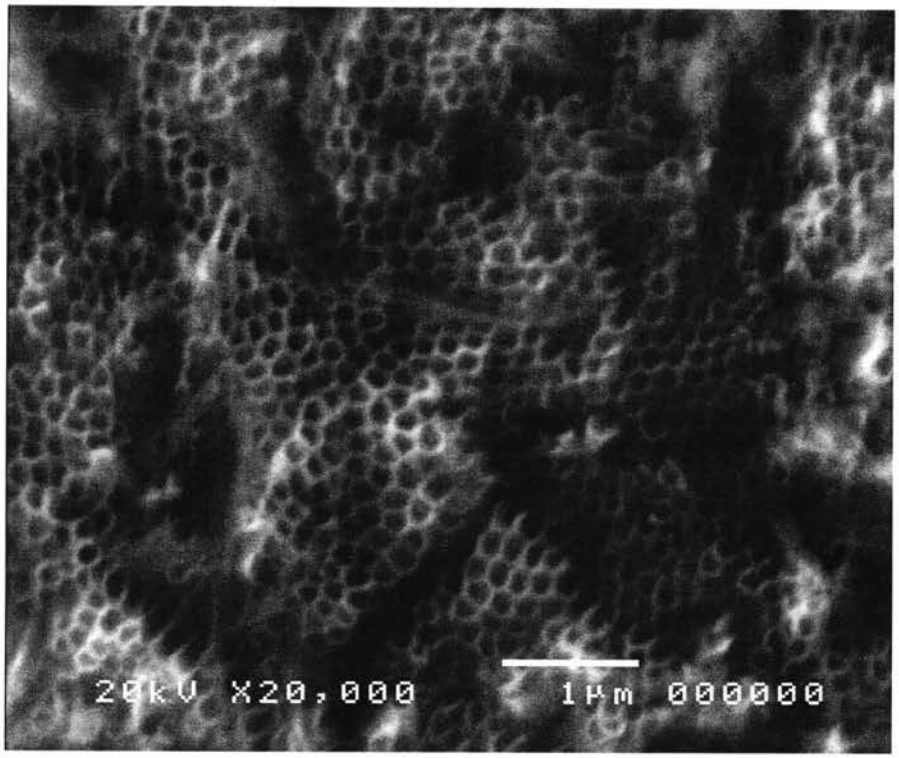

Figure 4.7 SEM image of TiO_2 nanotube arrays at 60 V.

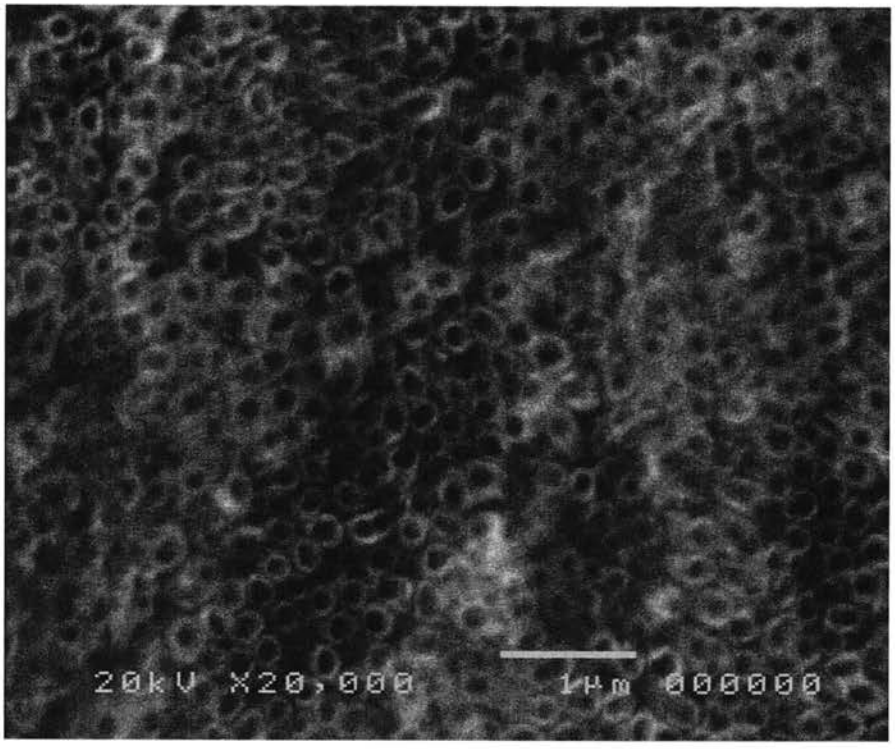

Figure 4.8 SEM image of TiO_2 nanotube arrays at 70 V.

The dye absorption of the TiO_2 nanotubes with various pore diameters was characterized with the UV-visible spectroscopy. The amount of absorbed dye solution is an important factor during the determination of energy conversion efficiency since the electrons are ejected only through the dyes attached to the TiO_2 nanotubes. Figure 4.9 shows the amount of dye absorption of TiO_2 nanotubes. It can be seen that the amount of dye absorption increased with increasing the pore diameter of nanotube because larger surface area is beneficial for dye absorption, and surface area is the function of the pore-size nanotubes. Thus, we concluded that pore diameter of TiO_2 nanotube dominates the efficiency of dye-sensitized solar cells [65].

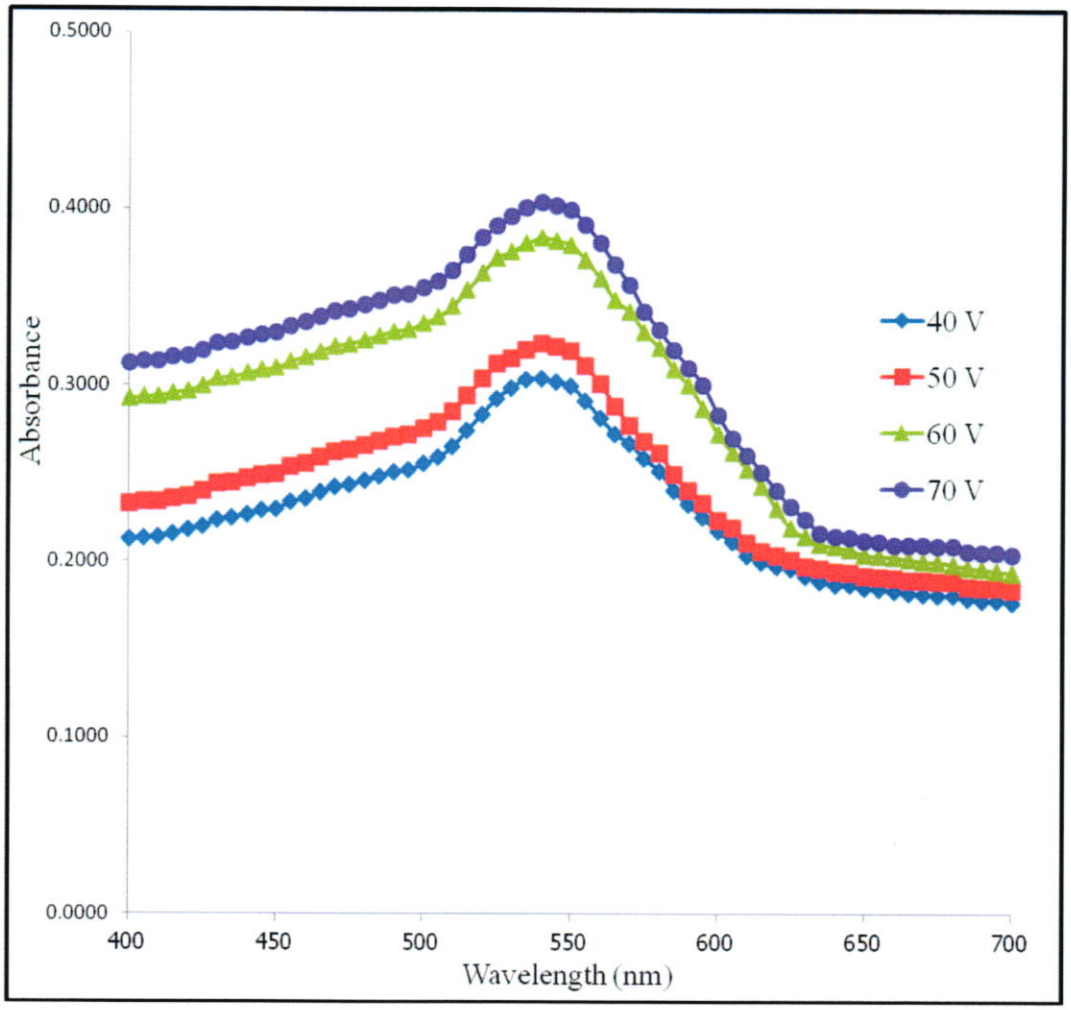

Figure 4.9 UV-vis spectra of TiO_2 nanotube arrays with various anodization voltages.

4.3 Solar cell performance

A number of researches demonstrate that self-organized TiO_2 array layers can enhance the light to electricity conversion efficiency of solar cells since the nanotubes has high surface area, strong internal light-scattering effect and facile charge transport. Here, the anodized TiO_2 nanotube arrays prepared at different applied voltage are used as photoanode for application in dye-sensitize solar cells [64].

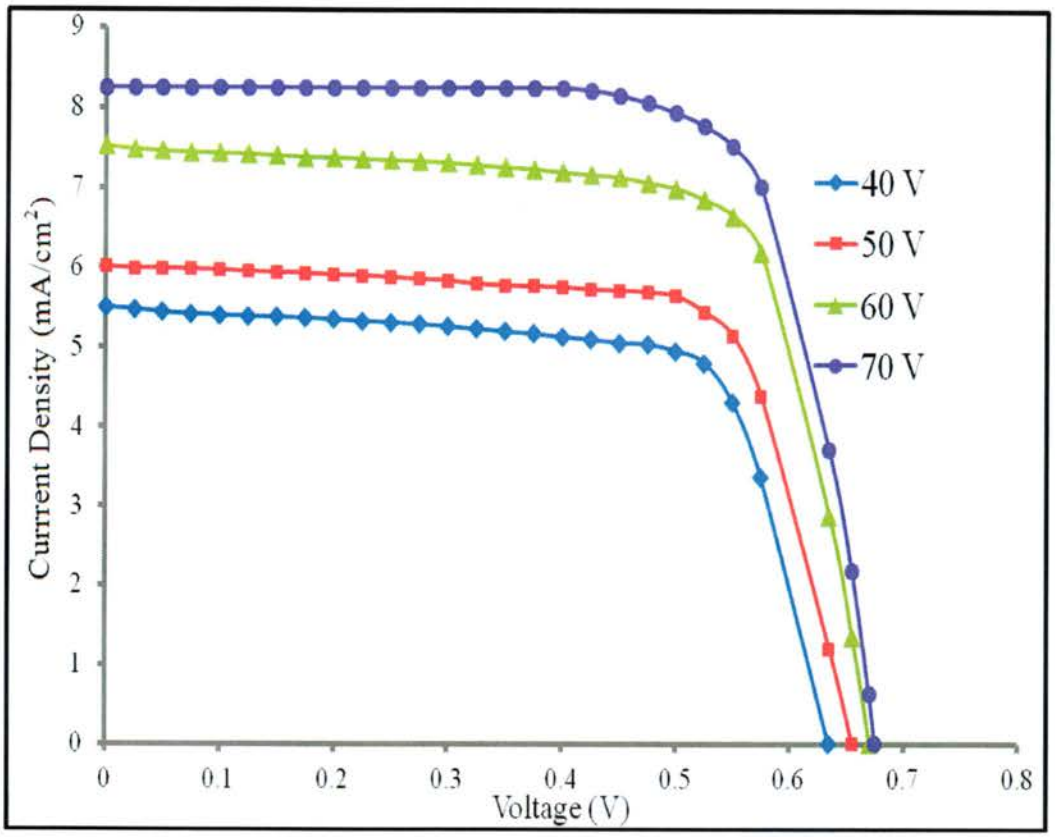

Figure 4.10 J–V characteristics of dye-sensitized solar cells based on different TiO_2 nanotube samples prepared at different applied voltages.

Figure 4.10 shows the photocurrent–voltage curves of DSSCs based on the N719 dye and organic electrolyte as a function of TiO_2 tube diameter under illumination of 60 mW/cm^2. The short circuit photocurrent densities (Jsc) obtained with TiO_2 nanotubes of 40, 50, 60 and 70 V anodization potential (or pore size of

nanotube of 90, 125, 150 and 200 nm) were 5.50, 6.01, 7.52 and 8.25 mA/cm^2 which the energy conversion efficiencies of dye-sensitized solar cells were 4.21, 4.77, 6.10 and 6.89% , respectively. The highest efficiency of 6.89% was achieved with TiO_2 nanotube arrays photoanode synthesized at 70V anodization potential. Detailed photovoltaic performance parameters (J_{sc}, V_{oc}, FF and η) of the DSSCs for films at different anodization potential were presented in Table 4.1. The energy conversion efficiency of the DSSCs increased with increasing pore size of nanotube (as a function of anodization potential). This is directly attributed to the increase in the amount of dye absorption form the increased surface area of film [6].

Table 4.1 Photovoltaic parameters of DSSCs based on four different TiO_2 nanotube samples prepared at different applied voltages.

Voltage (V)	**Anodization time (h)**	**Diameter (nm)**	J_{sc} **(mA/cm^2)**	V_{oc} **(V)**	FF	η (%)
40	5	90	5.50	0.635	0.72	4.21
50	5	125	6.01	0.655	0.73	4.77
60	5	150	7.52	0.665	0.73	6.10
70	5	200	8.25	0.675	0.74	6.89

CHAPTER 5
CONCLUSION AND SUGGESTIONS

We have synthesized and characterized of TiO_2 nanotubes by anodization method in mixed electrolytes at different pHs; 3 and 5. The morphology of the TiO_2 was found to be influenced by pH of the anodizing electrolytes. The prepared sample with the anodization in pH 5 electolyte was the titania films with anatase phase. The TiO_2 nanotubes were not observed while the samples with anodization in pH 3 electrolyte showed clearly titania nanotubes with diameters of about 100 nm. Then, we have succeeded in making TiO_2 nanotubes by anodization method in mixed electrolytes at voltages (40, 50, 60 and 70 V) and making dye-sensitized solar cell by using TiO_2 nanotubes as a working electrode. The corresponding average pore diameter of TiO_2 nanotubes is a function of the anodization voltage which the nanotube diameter increases as voltage increases. Furthermore, the TiO_2 nanotube diameters at applied voltage of 40, 50, 60 and 70 V were approximately 90, 125, 150 and 200 nm, respectively.

The anodized TiO_2 nanotube arrays prepared at different applied voltages are used as photoanodes for application in dye-sensitize solar cells. The photoconversion efficiencies of dye-sensitized solar cells made of the working electrodes obtained from of 40, 50, 60 and 70 V were 4.21%, 4.77%, 6.10% and 6.89% , respectively, under irradiation of 60 mW/cm^2. The highest efficiency of 6.89% was achieved with TiO_2 nanotube arrays working electrode synthesized at 70V anodization potential. The photoconversion efficiency of the DSSCs increases pore diameter of nanotube as a function of anodization potential increases. This is directly attributed by the increase of dye absorption form the increase of the surface area of the film. The greater the pore size and the greater the amount of dye absorbed, the better the electron transfer process leading to higher energy conversion efficiency of dye-sensitized solar cells.

In the future work, several conditions in the fabrication of TiO_2 nanotube arrays such as the effect of calcination temperature, different anodization times, water content and fluoride ion concentration will be investigated to improve the conversion

efficiency of TiO_2 nanotube dye-sensitize solar cells. In application, we may use TiO_2 nanotube arrays as photoanode for several devices such as dye-sensitize solar cells, hydrogen production and gas sensors.

REFERENCES

REFERENCES

[1] George W. Crabtree and et al. "The Hydrogen Economy", Physics today. 57(12): 39-44, 2004.

[2] Hongsik Choi and et al. "Review paper: Toward highly efficient quantum-dot- and dye-sensitized solar cells", Current Applied Physics xxx. 13(2): S2-S13, 2013.

[3] Md. K. Nazeeruddin , Etienne Baranoff and Michael Grätzel. "Dye-sensitized solar cells: A brief overview", Solar Energy. 85(6): 1172-1178, 2011.

[4] Hamid Omidvar and et al. "Influence of anodization parameters on the morphology of TiO_2 nanotube arrays", Superlattices and Microstructures. 50(1): 26-39, 2011.

[5] Xiaoyue Wang and et al. "Hydrothermal synthesis of well-aligned hierarchical TiO_2 tubular macrochannel arrays with large surface area for high performance dye-sensitized solar cells", Applied Energy. 99(C): 198-205, 2012.

[6] Rui Liu and et al. "Fabrication of TiO_2 nanotube arrays by electrochemical anodization in an NH_4F/H_3PO_4 electrolyte", Thin Solid Films. 519(19): 6459-6466, 2011.

[7] Hee Yeon Hwang and et al. "Influence of the organic electrolyte and anodization conditions on the preparation of well-aligned TiO_2 nanotube arrays in dye-sensitized solar cells", Solar Energy. 85(7): 1551-1559, 2011.

[8] Jung-Kun Lee and Mengjin Yang, "Progress in light harvesting and charge injection of dye-sensitized solar cells", Materials Science and Engineering. 176(15): 1142-1160, 2011.

[9] Jung Bing-Xin Lei and et al. "Fabrication of partially crystalline TiO_2 nanotube arrays using 1, 2-propanediol electrolytes and application in dye-sensitized solar cells", Advanced Powder Technology. 24(1): 175-182, 2013.

[10] J.J. Qiu, W.D. Yu, X.D. Gao and X.M. Li. "Sol–gel assisted ZnO nanorod array template to synthesize TiO_2 nanotube arrays", Nanotechnology. 17(18): 4695-4698, 2006.

REFERENCES (CONTINUED)

[11] F.W. Zhuge and et al. "Toward hierarchical TiO_2 nanotube arrays for efficient dye-sensitized solar cells", Advanced Materials. 23(11): 1330-1334, 2011.

[12] D. Gong and et al. "Titanium oxide nanotube arrays prepared by anodic oxidation", Materials Research. 16(12): 3331-3334, 2001.

[13] V. Galstyan and et al. "Fabrication of pure and Nb–TiO_2 nanotubes and their functional properties", Journal of Alloys and Compounds. 536(1): S488-S490, 2012.

[14] Shiqi Li and et al. "The role of the TiO_2 nanotube array morphologies in the dye-sensitized solar cells", Thin Solid Films. 520(2): 689-693, 2011.

[15] Pakawat wongwanwattana. Fabrication and photocatalysis of nanostructured TiO_2 for solar hydrogen production. Doctor's Thesis: Ubon Ratchathani University, 2011.

[16] Jacoboni and et al. "Review of Some Charge Transport Properties of Silicon", Solid State Electronics. 20(2): 77-89, 1977.

[17] Miguel Pelaez and et al. "A review on the visible light active titanium dioxide photocatalysts for environmental applications", Applied Catalysis B: Environmental. 125: 331-349, 2012.

[18] Mohamed AbdElmoula. Optical, Electrical and Catalytic Properties of Titania Nanotubes. Doctor's Thesis. Boston: Northeastern University, 2011.

[19] Yanjun Xin and et al. "Comparative study of photocatalytic and photoelectrocatalytic properties of alachlor using different morphology TiO_2/Ti photoelectrodes", Journal of Hazardous Materials. 192(3): 1812-1818, 2011.

[20] Gopal K. Mor and et al. "A review on highly ordered, vertically oriented TiO_2 nanotube arrays: Fabrication, material properties, and solar energy applications", Solar Energy Materials & Solar cells. 90(14): 2011-2075, 2006.

[21] G.A. Crawford and N. Chawla. "Porous hierarchical TiO_2 nanostructures: processing and microstructure relationships", Acta Materialia. 57(3): 854-867, 2009.

REFERENCES (CONTINUED)

[22] Dongliang Yu and ed al. "Morphological evolution of TiO_2 nanotube arrays with lotus-root-shaped nanostructure", Applied Surface Science. 276(1): 711-716, 2013.

[23] Chan Lin,Shougang Chen and Lixin Cao. "Anodic formation of aligned and bamboo-type TiO_2 nanotubes at constant low voltages", Materials Science in Semiconductor Processing. 16(1): 154-159, 2013.

[24] Chaorui Xue and et al. "Tailoring the surface morphology of TiO_2 nanotube arrays connected with nanowires by anodization", Materials Science in Semiconductor Processing. 14(2): 157-163, 2011.

[25] Dongsheng Guan, Paul J. Hymel and Ying Wang. "Growth mechanism and morphology control of double-layer and bamboo-type TiO_2 nanotube arrays by anodic oxidation", Electrochimica Acta. 83: 420-429, 2012.

[26] Lusheng Su and Yong X. Gan. "Formation and thermoelectric property of TiO_2 nanotubes covered by Te–Bi–Pb nanoparticles", Electrochimica Acta. 56(16): 5794-5803, 2011.

[27] Y.Q. Liang and et al. "Study on the formation micromechanism of TiO_2 nanotubes on pure titanium and the role of fluoride ions in electrolyte solutions", Thin Solid Films. 519(15): 5150-5155, 2011.

[28] H. Liu, L. Tao and W.Z. Shen. "Optimal self-organized growth of small anodic TiO_2 nanotubes with "micro-annealing" effect under complex conditions via reaction–diffusion approach", Electrochimica Acta. 56(11): 3905-3913, 2011.

[29] Jung Gyu Nam and et al. "Enhancement of the efficiency of dye-sensitized solar cell by utilizing carbon nanotube counter electrode", Solar Scripta Materialia. 62(3): 148-150, 2010.

[30] J.M. Macak and et al. "Mechanistic aspects and growth of large diameter self-organized TiO_2 nanotubes", Journal of Electrochemisty. 621(2): 245-266, 2008.

[31] Pacharee Krongkitsiri. Synthesis and Characterization of nanostructured TiO_2 for solar hydrogen. Doctor's Thesis: Ubon Ratchathani University, 2010.

REFERENCES (CONTINUED)

[32] Jae Sung Yun. Mechanisms of TiO_2 Nanotube Fabrication by Anodisation. Doctor's Thesis, Wales, The University of New South Wales, 2010

[33] Poulomi Roy and et al. "TiO_2 nanotubes and their application in dye-sensitized solar cells", Nanoscale. 2(1): 45-59, 2010.

[34] Zhang Lan and et al. "Quasi-solid state dye-sensitized solar cells based on gel polymer electrolyte with poly(acrylonitrile-co-styrene)/NaI+I_2", Solar Energy. 80(11): 1483-1488, 2006.

[35] Hongxun Yang and et al. "The polymer gel electrolyte based on poly(methyl methacrylate) and its application in quasi-solid-state dye-sensitized solar cells", Materials Chemistry and Physics. 110(1): 38-42, 2008.

[36] S. Anandan "Recent improvements and arising challenges in dye-sensitized solar cells", Solar Energy Materials and Solar Cells. 91(9): 843-846, 2007.

[37] Qifeng Zhang and Guozhong Cao. "Nanostructured photoelectrodes for dye-sensitized solar cells", Nano Today. 6(1): 91-109, 2011.

[38] A. Kay and M. Gratzel. "Low cost photovoltaic modules based on dye sensitized nanocrystalline titanium dioxide and carbon powder", Solar Energy Materials and Solar Cells. 44(1): 99-117, 1996.

[39] Laura L. Tobin and et al. "Characterising dye-sensitised solar cells", Optik. 122(14): 1225-1230, 2011.

[40] F. Odobel, E. Blart and M. Lagree. "Porphyrin dyes for TiO_2 sensitization," Journal of Materials Chemistry. 13(1): 502–510, 2003.

[41] M. K. Nazeeruddin, R. Humphry-Baker and M. Gratzel."Efficient near-IR sensitization of nanocrystalline TiO_2 films by zinc and aluminum phthalocyanines", Journal of Porphyrins and Phthalocyanines. 3(3): 230-237, 1999.

[42] J. He, A. Hagfeldt and S. E. Lindquist. "Phthalocyanine sensitized Nanostructured TiO_2 electrodes prepared by a novel anchoring method", Langmuir. 17(9): 2743-2747, 2001.

[43] W. Paw and et al. "Luminescent platinum complexes: tuning and using the excited state", Coordination Chemistry Reviews. 171(1): 125-150, 1998.

REFERENCES (CONTINUED)

[44] A. Islam, H. Sugihara and K. Hara. "Dye sensitization of nanocrystalline titanium dioxide with square planar platinum(II) diimine dithiolate complexes", Inorganic Chemistry. 40(21): 5371–5380, 2001.

[45] J. M. Rehm and et al. "Femtosecond electron-transfer dynamics at a sensitizing dye-semiconductor (TiO_2) interface", Journal of Physical Chemistry. 100(23): 9577-9578, 1996.

[46] P. V. Kamat and W. E. Ford, "Photochemistry on surfaces: triplet-triplet energy transfer on colloidal TiO_2 particles", Chemical Physics Letters. 135(4-5): 421-426, 1987.

[47] S. Das, C. S. Rajesh and C. H. Sureshl. "Photophysical and photoelectrochemical behavior of poly[styrene-co-3-(acrylamido)-6-aminoacridine", Macromolecules. 28(12): 4249-4254, 1995.

[48] J. Bisquert and et al. " Physical chemical principles of photovoltaic conversion with nanopartuculate, mesoporous dye-sensitized solar cells", Journal of Physical Chemistry. 108(24): 8106 -8118, 2004.

[49] Wu and et al. "Progress on the electrolytes for dye-sensitized solar cells", Pure and Applied Chemistry. 80(11): 2241-2258, 2008.

[50] Ferber J, Stangl R and Luther J. "An electrical model of the dye-sensitized solar cell", Solar Energy Materials and Solar Cells. 53(1-2): 29-54, 1998.

[51] Lin CK and et al. "Characterization of electrophoretically deposited nanocrystalline titanium dioxide films", Surface and Coating Technology. 200(10): 3184-3189, 2006.

[52] Ajay Jena and et al. "Dye Sensitized Solar Cells: A review", Transactions of the Indian Ceramic Society. 71(1): 1-16, 2012.

[53] R.V.M. Otakwa and et al. "Application of Dye-Sensitized Solar Cell Technology in the Tropics: Effects of Air Mass on Device Performance", International Journal of Renewable Energy Research. 2(3): 369-375, 2004.

REFERENCES (CONTINUED)

[54] Md. K. Nazeeruddin and et al. "A high molar extinction coefficient charge transfer sensitizer and its application in dye-sensitized solar cell", Journal of Photochemistry and Photobiology A: Chemistry. 185(2-3): 331-337, 2007.

[55] Janne Halme. Dye-sensitized nanostructured and organic photovoltaic cells: technical review and preliminary tests. Doctor's Thesis, Helsinki University of Technology, 2002

[56] Jihuai Wu and et al. "Gel polymer electrolyte based on poly(acrylonitrile-*co*-styrene) and a novel organic iodide salt for quasi-solid state dye-sensitized solar cell", Electrochimica Acta. 51(20): 4243-4249, 2006.

[57] T. Miyamoto and K. Shibayama, "Free-volume model for ionic conductivity in polymers", Journal of Applied Physics. 44(12): 5372-5376, 1973.

[58] Greg P. Smestad. "Education and solar conversion:Demonstrating electron transfer", Solar Energy Materials and Solar Cells. 55(1-2): 157-178, 1998.

[59] P. Li and et al. "High performance and low platinum loading Pt/carbon black counter electrode for dye-sensitized solar cells", Solar Energy. 83(6): 845-849, 2009

[60] Soon Hyung Kang and et al. "Formation and mechanistic study of self-ordered TiO_2 nanotubes on Ti substrate", Journal of Industrial and Engineering Chemistry. 14(1): 52-59, 2008.

[61] Srimala Sreekantan, Roshasnorlyza Hazan and Zainovia Lockman."Photoactivity of anatase–rutile TiO_2 nanotubes formed by anodization method", Thin Solid Films. 518(1): 16-21, 2009.

[62] Qi Pang and et al. "Dye sensitized solar cells using freestanding TiO_2 nanotube arrays on FTO substrate as photoanode", Materials Chemistry and Physics. 125(3): 612-616, 2011.

[63] Yan Grzegorz D. Sulka and et al. "Fabrication of nanoporous TiO_2 by Electrochemical anodization", Electrochimica Acta. 55(14): 4359-4367, 2010.

REFERENCES (CONTINUED)

[64] S. Agarwala and G.W. Ho. "Self-ordering anodized nanotubes: Enhancing the performance by surface plasmon for dye-sensitized solar cell", Journal of Solid State Chemistry. 189: 101-107, 2012.

[65] Jian-Yang Lin, Ting-Jia Chen and Chih-Kai Hu. "Effects of Anodic Titanium Oxide Nanotube arrays on dye-sensitized solar cells", Journal of the Chinese Chemical Society. 57(5B): 1176-1179, 2010.

APPENDIX

PUBLICATION/PROCEEDINGS

1. **S. Wantawee**, P. Krongkitsiri, T. Saipin, B. Samran and U. Tipparach. "Synthesis and Structure of Titania Nanotubes for Hydrogen Generation", Advanced Materials Research. 741: 84-89, 2013.
2. T. Saipin, **S. Wantawee** and U. Tipparach. "Efficiency of Dye-Sensitized Solar Cells Based on Carbon Nanotubes and TiO_2 Nanocystalline", Proceedings of the 7th Annual conference of Thai Physics Society, SPC 2012: Organized by Ayuthaya, Thailand, Pages 98-101.
3. B. Samran, P. Krongkitsiri, T. Saipin, **S. Wantawee**, S. Budngam and U. Tipparach. "Fabrication and Characterization anodized Titania Nanotubes for enhancing hydrogen generation", Proceedings of the 8th Annual conference of Thai Physics Society, SPC 2013: Organized by Chiang Mai, Thailand, Pages 255-258.